

## Supporting Information

### **Triphenylamine-equipped 1,8-naphthoalactam: A versatile scaffold for the custom design of efficient subcellular imaging agents**

Yingzhong Li,<sup>‡</sup> Lizhen Chen,<sup>‡</sup> Leilei Si, Yang, Yang, Chunlei Zhou, Fuqing Yu, Guomin Xia,<sup>\*</sup> and Hongming Wang,<sup>\*</sup>

Institute for Advanced Study and College of Chemistry, Nanchang University, 999 Xuefu Road, Nanchang, 330031, P. R. China.

E-mail: [guominxia@ncu.edu.cn](mailto:guominxia@ncu.edu.cn), [hongmingwang@ncu.edu.cn](mailto:hongmingwang@ncu.edu.cn).

<sup>‡</sup> Corresponding author.

<sup>‡</sup> Y.L. and L.C. contributed equally to this work.

## Contents

<b>1. Materials and Instruments</b> .....	3
<b>2. Cell culture and viability assay</b> .....	3
<b>3. Incubation of dyes and cell fluorescence imaging</b> .....	3
<b>4. Synthesis</b> .....	4
4.1 Synthesis of precursor 2 .....	4
4.2 Synthesis of precursor 3 .....	4
4.3 Synthesis of NP-TPA-Lyso .....	5
4.4 Synthesis of NP-TPA-Mito .....	5
4.5 Synthesis of NP-TPA-ER .....	6
4.6 Synthesis of NP-TPA-CM .....	6
<b>5. Spectral properties</b> .....	8
<b>6. Cytotoxicity</b> .....	13
<b>7. Cellular imaging</b> .....	14
<b>8. The characterization of <math>^1\text{H}</math> NMR, <math>^{13}\text{C}</math> NMR, and mass spectra</b> .....	20
<b>9. References</b> .....	28

## 1. Materials and Instruments.

1,8-naphthoalactam, bis(pinacolato)diboron, 1,3-dibromopropane, triphenylphosphine, morpholine, 4-methylbenzenesulfonamide, trimethylamine, and other materials were purchased from commercial suppliers and used without further purification unless explicitly stated. The commercial dyes were bought from Beyotime Biotechnology. NMR spectra of  $^1\text{H}$  NMR and  $^{13}\text{C}$  NMR spectra were recorded on a Bruker AVANCE 400 spectrometer and using tetra-methylsilane (TMS) as the internal standard. Mass spectra were obtained with Trip TOFTM 5600 mass spectrometers. UV-visible absorption spectra were acquired on a Lambda 750 spectrophotometer. Photoluminescence (PL) spectra were recorded on a Horiba FluoroMax-4 luminescence spectrometer. The absolute fluorescence quantum yield ( $\Phi_{\text{PL}}$ ) was determined using a Horiba FL-3018 Integrating Sphere. The fluorescence lifetime measurement was performed on a Horiba FluoreCube spectro-fluorometer system using a UV diode laser (NanoLED 390 nm) for excitation. All the imaging and photostability cell imaging data were taken under the light-shielded condition on a laser confocal microscope Zeiss LSM710.

## 2. Cell culture and viability assay

Hep G2 and HUVEC cells were cultured in Dulbecco's modified Eagle's medium (DMEM) with 10% FBS and a 90% relative humidity containing 5%  $\text{CO}_2$  at 37 °C. The viability assay of NP-TPA-Tar was estimated by an MTT assay in vitro. Normal and cancer cells were chosen (HUVEC and Hep G2) with a density of  $1 \times 10^4$  cells per well in 96-well plates and incubated overnight. Then, cultured with various concentrations of probes for another 24 h in darkness and treated with CCK-8 for another 2 h. The cell viability assay was obtained according to the method of the previously reported literature <sup>1</sup>.

## 3. Incubation of dyes and cell fluorescence imaging

Hep G2 cells were cultured in DMEM medium according to the above culture conditions and transferred into confocal dishes with a diameter of 35 mm for growth overnight. The stock solutions of NP-TPA-Tars was prepared with dimethyl sulfoxide at a concentration of 1mM. The next day, co-incubation of NP-TPA-Tar and commercial dye with Hep G2 cells according to the experimental scheme to determine the incubation concentration and time. Note that the HBSS culture medium was used for endoplasmic reticulum targeted imaging. After that, remove dye working solution and wash the confocal dishes three times with a cell culture medium. The

confocal dish was positioned on glass slides of a laser confocal microscope (Zeiss LSM710) to image by using a 40x objective. The overlap coefficient analysis was conducted in ZEN software.

## 4. Synthesis

### 4.1 Synthesis of precursor 2

The synthesis steps of precursor 1 are shown in Scheme 1. For the specific procedure, refer to our previously published literature <sup>2</sup>. To a solution of the precursor 1 (2.36 g, 8 mmol), 4-bromo-N,N-diphenylaniline (3.11 g, 9.6 mmol), cesium carbonate (13 g, 40 mmol), tetrakis (triphenylphosphine) palladium (461 mg, 0.4 mmol) in dioxane (100 mL) with water (10 mL) and stirring at 95 °C under N<sub>2</sub> atmosphere for 12 h. Then the solvent was removed under reduced pressure, and the residue was extracted with ethyl acetate and water. The organic layer was retained and dried over Na<sub>2</sub>SO<sub>4</sub>. The obtained crude product was purified by silica gel column chromatography using petroleum ether/ethyl acetate (10 / 1) as the eluent to afford a light red solid (2.37 g, 72 %). <sup>1</sup>H NMR (400 MHz, DMSO-d<sub>6</sub>, δ): 10.84 (s, 1H), 8.17 (d, J = 8.27 Hz, 1H), 8.04 (d, J = 6.95 Hz, 1H), 7.81 (t, J = 7.62 Hz, 1H), 7.39 (t, J = 15.36, 3H), 7.39 (t, J = 15.36, 3H), 7.33 (t, J = 7.68 Hz, 4H), 7.06 (m, 9H). <sup>13</sup>C NMR (100 MHz, DMSO-d<sub>6</sub>, δ): 169.16, 147.49, 146.94, 137.72, 132.90, 132.50, 130.93, 130.10, 130.01, 129.71, 129.19, 127.69, 127.63, 126.28, 124.67, 124.28, 123.74, 123.43, 123.38, 109.98, 106.88.

### 4.2 Synthesis of precursor 3

To acetonitrile (50 mL) was added precursor 2 (2.06 g, 5 mmol) and potassium carbonate (1.03 g, 7.5 mmol). The mixture was stirred, and 1,3-Dibromopropane (10.1 g, 50 mmol) was added. After stirring for 5 h at 85 °C, the mixture was filtered to remove potassium carbonate, and the solvent was removed under reduced pressure. Then the crude product was purified by silica gel column chromatography using petroleum ether/ethyl acetate (50 / 1) as the eluent to afford an orange-yellow solid (1.39 g, 52 %). <sup>1</sup>H NMR (400 MHz, DMSO-d<sub>6</sub>) δ 2.28 (p, J = 6.7 Hz, 2H), 3.61 (t, J = 6.6 Hz, 2H), 4.04 (t, J = 6.9 Hz, 2H), 7.06 – 7.14 (m, 8H), 7.28 (d, J = 7.4 Hz, 1H), 7.32 – 7.38 (m, 4H), 7.46 – 7.50 (m, 2H), 7.53 (d, J = 7.4 Hz, 1H), 7.83 (dd, J = 8.4, 7.0 Hz, 1H), 8.10 (d, J = 6.9 Hz, 1H),

8.20 (d,  $J = 8.3$  Hz, 1H).  $^{13}\text{C}$  NMR (101 MHz, dmsO)  $\delta$  31.56, 31.81, 38.39, 38.89, 39.10, 39.31, 39.52, 39.73, 39.94, 40.14, 105.87, 122.93, 123.29, 124.24, 124.61, 126.20, 126.93, 128.54, 129.27, 130.49, 132.35, 132.78, 137.96, 146.60, 147.02, 166.90. TOF MS:  $m/z$ : calcd. for [precursor 3 + H] $^+$ : 533.1223; found: 533.1212.

### 4.3 Synthesis of NP-TPA-Lyso

To a solution of acetonitrile (50 mL) was added the precursor 3 (1.07 g, 2 mmol), potassium carbonate (414 mg, 3 mmol), morpholine (1.74 g, 20 mmol) and stirred at 85 °C for 24 h. The mixture was filtered to remove potassium carbonate, and the solvent was removed under reduced pressure. Then the crude product was purified by silica gel column chromatography using petroleum ether/ethyl acetate (20 / 1) as the eluent to afford an orange solid (0.67 g, 62 %).  $^1\text{H}$  NMR (400 MHz,  $\text{DMSO-}d_6$ )  $\delta$  8.14 (d,  $J = 8.3$  Hz, 1H), 8.03 (d,  $J = 6.9$  Hz, 1H), 7.76 (dd,  $J = 8.3, 7.0$  Hz, 1H), 7.44 (dd,  $J = 12.8, 7.9$  Hz, 3H), 7.30 (dd,  $J = 8.4, 7.2$  Hz, 4H), 7.20 (d,  $J = 7.4$  Hz, 1H), 7.06 (dt,  $J = 6.7, 3.5$  Hz, 8H), 3.91 (t,  $J = 6.7$  Hz, 2H), 3.42 (s, 4H), 2.31 (d,  $J = 6.4$  Hz, 2H), 2.25 (s, 4H), 1.83 (p,  $J = 6.8$  Hz, 2H).  $^{13}\text{C}$  NMR (101 MHz, dmsO)  $\delta$  25.31, 38.38, 53.62, 55.84, 66.45, 106.39, 123.44, 123.71, 124.42, 124.65, 125.06, 126.88, 127.33, 129.00, 129.61, 130.04, 130.92, 132.89, 132.98, 138.77, 147.01, 147.49, 167.41. TOF MS:  $m/z$ : calcd. for [NP-TPA-Lyso + H] $^+$ : 540.2646; found: 540.2643.

### 4.4 Synthesis of NP-TPA-Mito

To a solution of toluene (50 mL) was added the precursor 3 (1.07 g, 2 mmol) and triphenylphosphine (1.57 g, 6 mmol) and stirred at 120 °C for 12 h. The mixture was cooled to room temperature, and the obtained precipitates were then filtered and recrystallized in toluene to afford pure yellow crystals (1.29 g, 81 %).  $^1\text{H}$  NMR (400 MHz,  $\text{DMSO-}d_6$ )  $\delta$  8.17 (dd,  $J = 8.3, 2.1$  Hz, 1H), 8.05 (dd,  $J = 7.0, 2.1$  Hz, 1H), 7.85 (td,  $J = 7.0, 3.3$  Hz, 3H), 7.82 – 7.74 (m, 6H), 7.74 – 7.66 (m, 6H), 7.47 (td,  $J = 8.4, 7.8, 2.2$  Hz, 4H), 7.33 (td,  $J = 7.9, 7.2, 2.1$  Hz, 4H), 7.26 (dd,  $J = 7.4, 2.2$  Hz, 1H), 7.08 (qd,  $J = 9.7, 9.2, 4.6$  Hz, 8H), 4.13 (t,  $J = 6.9$  Hz, 2H), 3.80 (td,  $J = 11.6, 8.2, 4.3$  Hz, 2H), 2.03 (q,  $J = 7.7$  Hz, 2H).  $^{13}\text{C}$  NMR (101 MHz, dmsO)  $\delta$  18.52, 19.03, 21.88, 106.41, 118.27, 119.14, 123.42, 123.80, 124.71, 125.18, 126.77, 127.39, 128.93, 129.74, 130.10, 130.60, 130.72, 130.98, 132.80,

133.27, 134.05, 134.15, 135.38, 138.33, 147.08, 147.48, 167.51. TOF MS: m/z: calcd. for [NP-TPA-Mito]<sup>+</sup>: 715.2873; found: 715.2867.

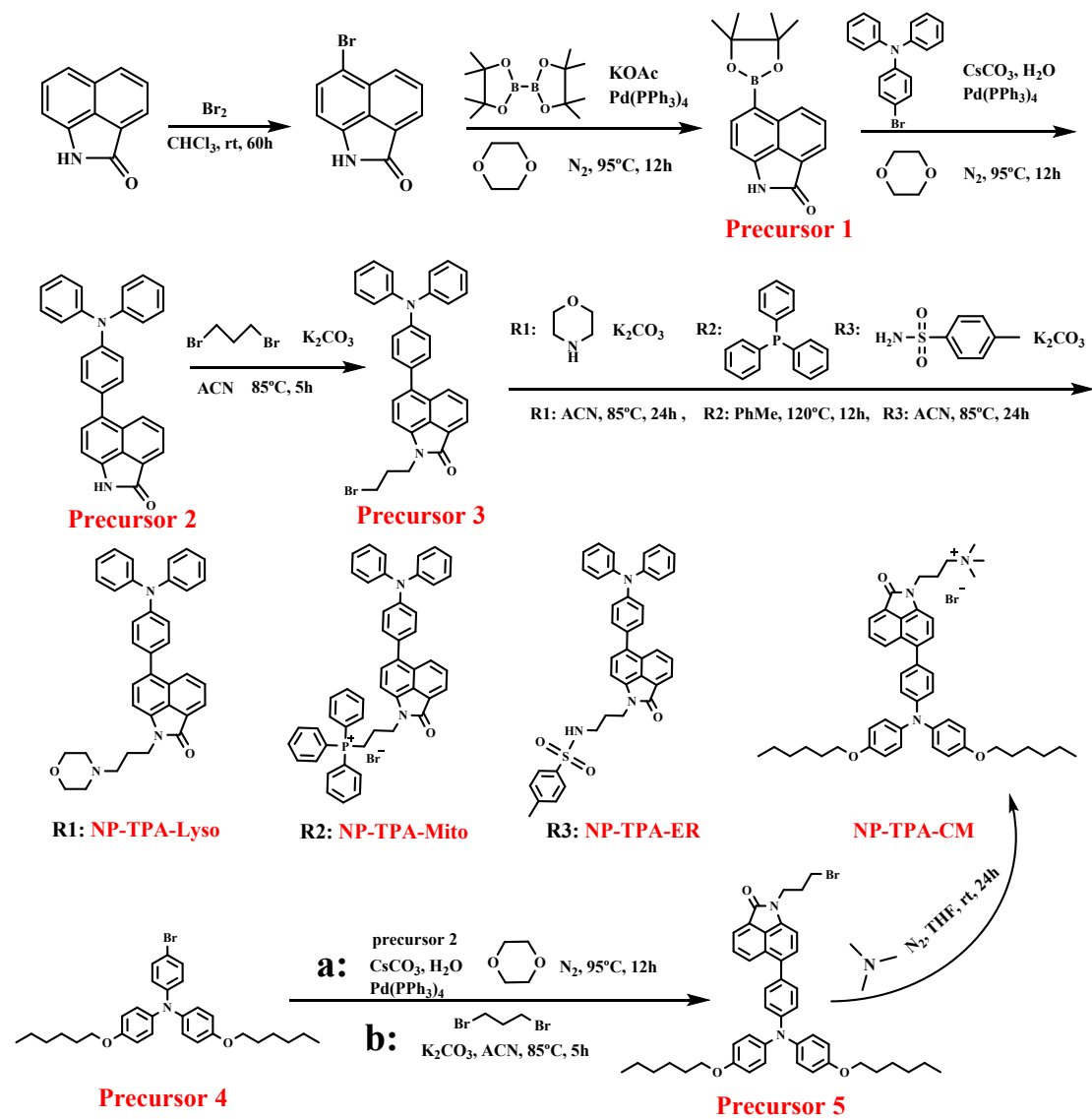
#### 4.5 Synthesis of NP-TPA-ER

To a solution of acetonitrile (50 mL) was added precursor 3 (1.07 g, 2 mmol), 4-methylbenzenesulfonamide (1.03 g, 6 mmol), and potassium carbonate (0.41 g, 3 mmol), and stirred at 85°C for 24 h. The mixture was then filtered to remove potassium carbonate, and the solvent was removed under reduced pressure. The crude product was purified by silica gel column chromatography using petroleum ether/ethyl acetate (4 / 1) as the eluent to afford an orange solid (0.91 g, 73 %). <sup>1</sup>H NMR (400 MHz, DMSO-*d*<sub>6</sub>) δ 8.15 (d, *J* = 8.3 Hz, 1H), 8.04 (d, *J* = 7.0 Hz, 1H), 7.78 (dd, *J* = 8.3, 7.0 Hz, 1H), 7.64 – 7.56 (m, 3H), 7.46 (dd, *J* = 7.9, 3.9 Hz, 3H), 7.34 – 7.30 (m, 3H), 7.28 (d, *J* = 8.0 Hz, 3H), 7.17 (d, *J* = 7.4 Hz, 1H), 7.08 (dt, *J* = 7.0, 5.3 Hz, 7H), 3.86 (t, *J* = 7.1 Hz, 2H), 2.84 (s, 2H), 2.34 (d, *J* = 3.3 Hz, 1H), 2.29 (s, 3H), 1.80 (p, *J* = 7.2 Hz, 2H). <sup>13</sup>C NMR (101 MHz, dms) δ 21.36, 25.40, 28.85, 37.75, 106.43, 123.42, 123.75, 124.59, 124.68, 124.95, 126.06, 126.59, 126.93, 127.33, 128.97, 129.72, 130.01, 130.19, 130.95, 132.83, 133.17, 137.75, 138.31, 143.00, 147.05, 147.49, 167.24. TOF MS: m/z: calcd. for [NP-TPA- ER + H]<sup>+</sup>: 624.2316; found: 624.2286.

#### 4.6 Synthesis of NP-TPA-CM

The precursor 4 was obtained by the synthetic method of M. F. Shah et al.<sup>3</sup>. Following the synthesis steps of precursors 2 and 3, precursor 5 can be prepared. Under N<sub>2</sub> atmosphere, the trimethylamine solution (5 mL, 2 mol/L in THF) was added dropwise into a solution of precursor 5 (1.47 g, 2 mmol) in THF (50 mL). The mixture was stirred at 25 °C for 24 h and the solvent was then removed under reduced pressure. The crude product was purified by silica gel column chromatography using dichloromethane / methanol (10 / 1) as the eluent to afford an orange solid (1.39 g, 88 %). <sup>1</sup>H NMR (400 MHz, DMSO-*d*<sub>6</sub>) δ 8.15 (d, *J* = 8.3 Hz, 1H), 8.07 (d, *J* = 6.9 Hz, 1H), 7.79 (t, *J* = 7.7 Hz, 1H), 7.47 (d, *J* = 7.4 Hz, 1H), 7.34 (dd, *J* = 7.8, 5.1 Hz, 3H), 7.05 (d, *J* = 8.7 Hz, 4H), 6.88 (t, *J* = 8.2 Hz, 6H), 3.99 (t, *J* = 6.6 Hz, 2H), 3.90 (t, *J* = 6.4 Hz, 4H), 3.53 – 3.44 (m, 2H), 3.06 (s, 9H), 2.18 (p, *J* = 6.9 Hz, 2H), 1.66 (p, *J* = 6.8 Hz, 4H), 1.37 (p, *J* = 7.0, 6.6 Hz, 4H), 1.26 (h, *J* = 3.8 Hz, 8H), 0.85 (d, *J* = 6.4 Hz, 6H). <sup>13</sup>C NMR (101 MHz, dms) δ 14.35, 22.52, 22.74, 25.66, 29.16, 31.45, 37.33,

52.74, 63.47, 68.08, 106.67, 115.96, 119.37, 124.64, 125.15, 126.58, 127.39, 127.50, 128.65, 129.63, 130.12, 130.61, 133.73, 137.87, 140.19, 148.33, 155.84, 167.48. TOF MS: m/z: calcd. for [NP-TPA-CM]<sup>+</sup>: 712.4473; found: 712.4476.



Scheme S1. Synthesis scheme of NP-TPA-Tars.

## 5. Spectral properties

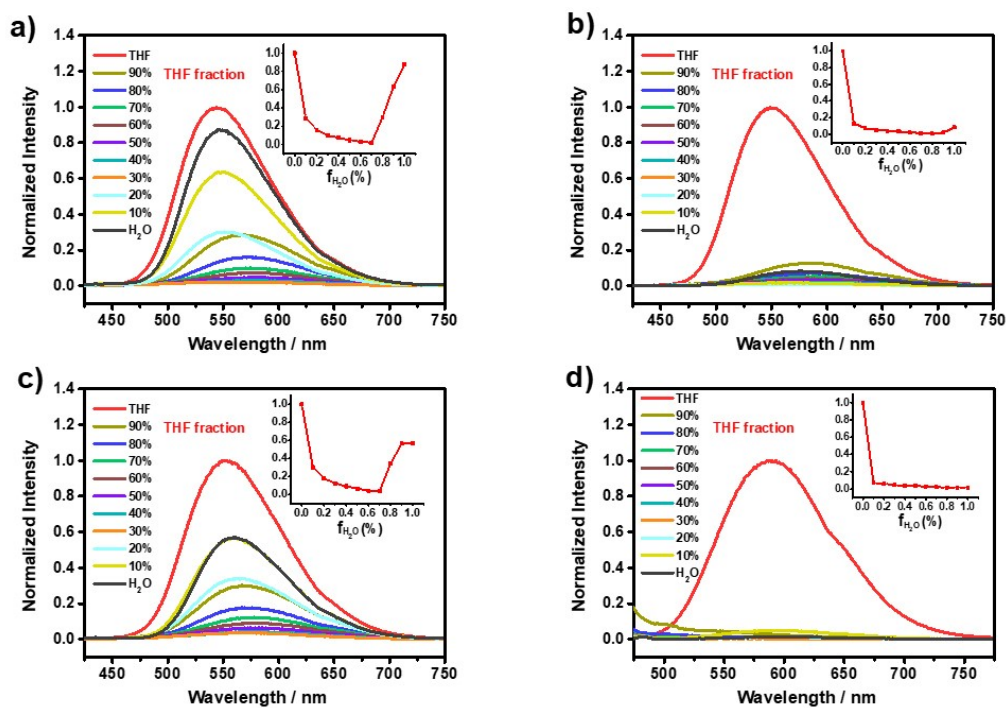


Fig. S1 The fluorescence emission changes of NP-TPA-Tars (10  $\mu$ M,  $\lambda_{ex}$  = 405 nm) in THF solutions with different fractions of water ( $f_w$ ) at room temperature. Insert: the emission trend diagram with different  $f_w$ . (a) NP-TPA-Lyso, (b) NP-TPA-Mito, (c) NP-TPA-ER, (d) NP-TPA-CM.



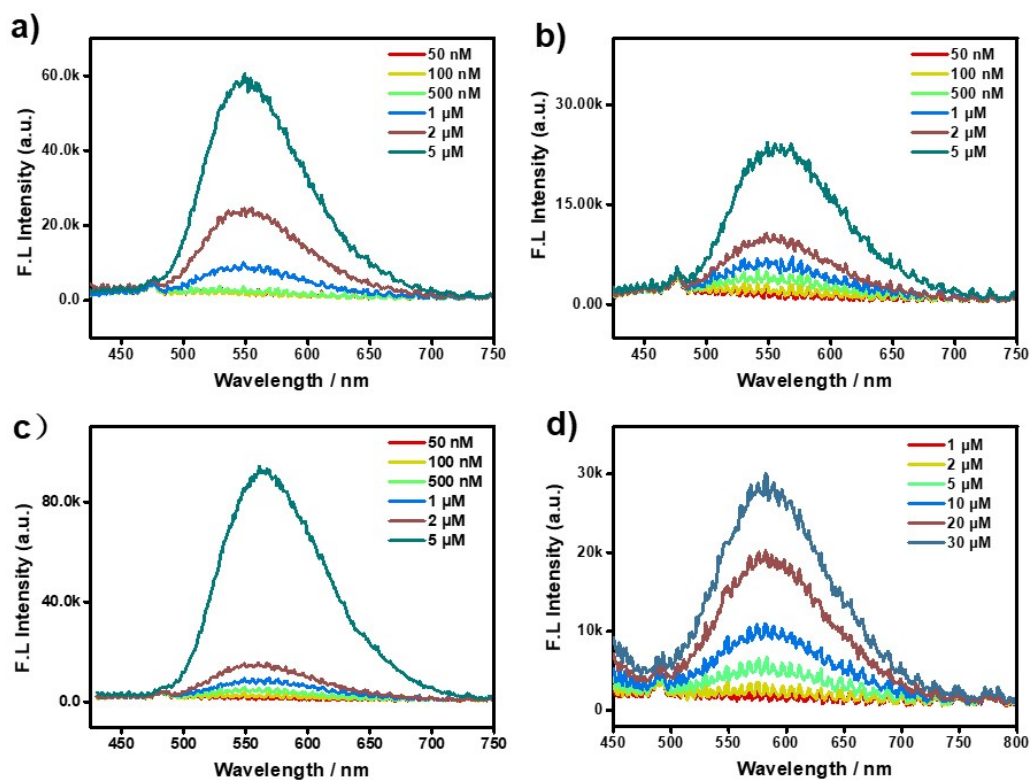


Fig. S2 The fluorescence emission of NP-TPA-Tars ( $\lambda_{\text{ex}} = 405 \text{ nm}$ ) in PBS solution with different concentrations at room temperature. (a) NP-TPA-Lyso, (b) NP-TPA-Mito, (c) NP-TPA-ER and (d) NP-TPA-CM.

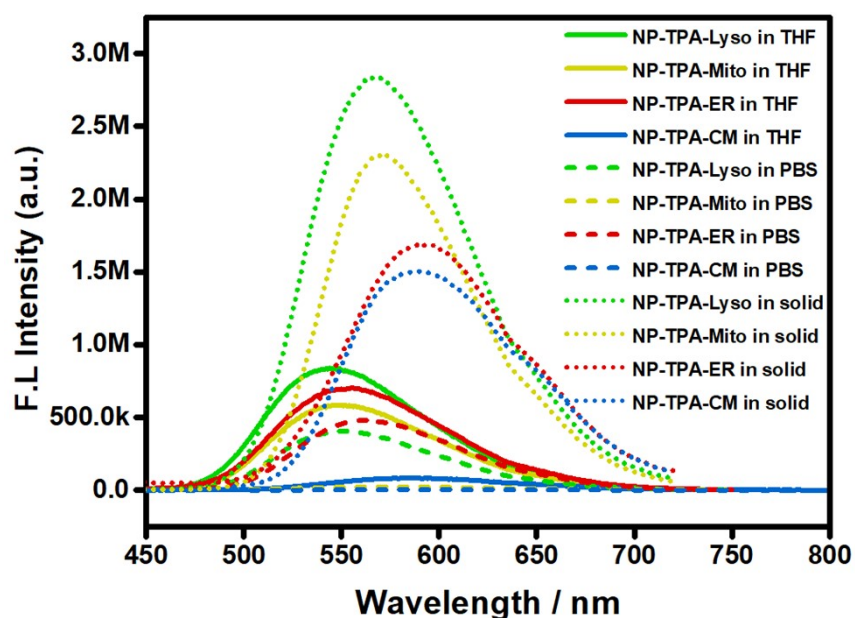


Fig. S3 The fluorescence emission of NP-TPA-Tars (10  $\mu$ M,  $\lambda_{\text{ex}} = 405 \text{ nm}$ , slit: 2nm) in THF (solid line), in PBS (short dash) and in solid state (short dash dot), respectively.

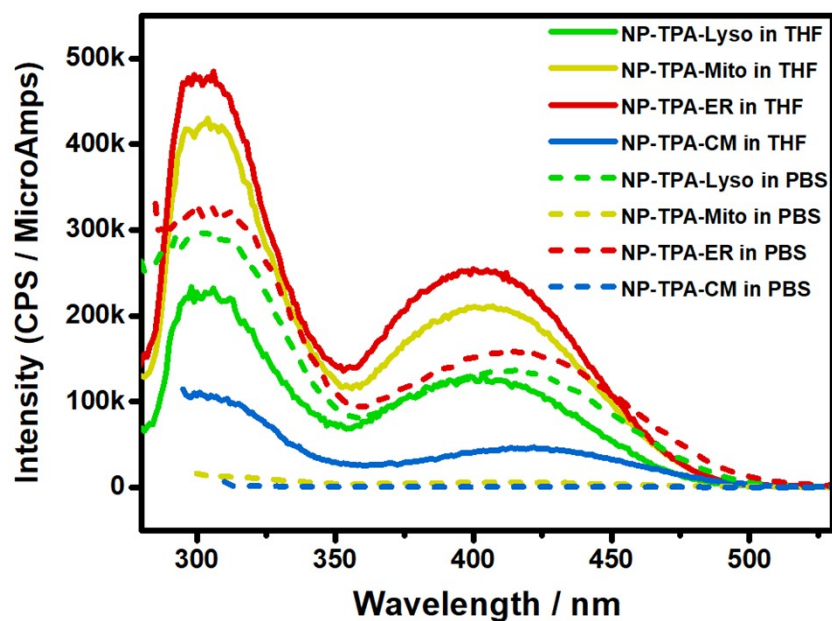


Fig. S4 Excitation spectrum of NP-TPA-Tars (10  $\mu$ M, slit: 2nm) in THF (solid line) and in PBS (short dash).

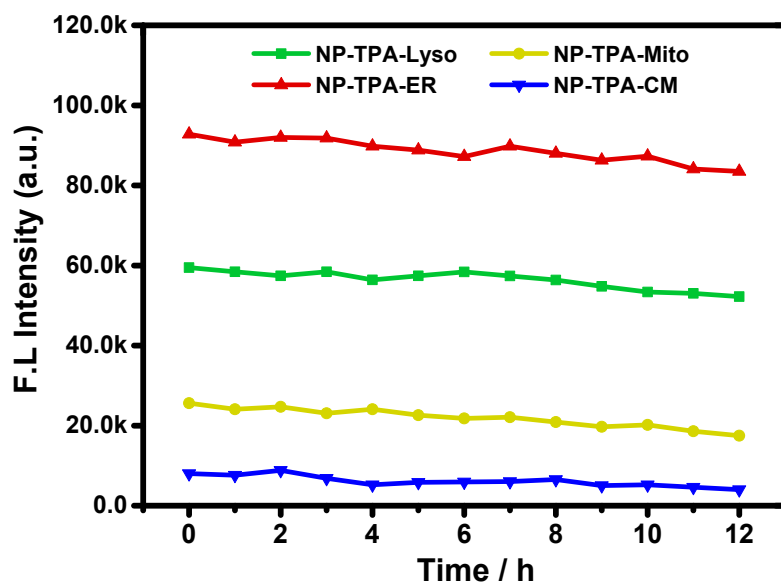


Fig. S5 The fluorescence emission tendency of NP-TPA-Tars (5  $\mu$ M,  $\lambda_{ex}$  = 405 nm) in cell culture fluid except that NP-TPA-ER in HBSS within 12 hours at room temperature. (a) NP-TPA-Lyso, (b) NP-TPA-Mito, (c) NP-TPA-ER and (d) NP-TPA-CM.

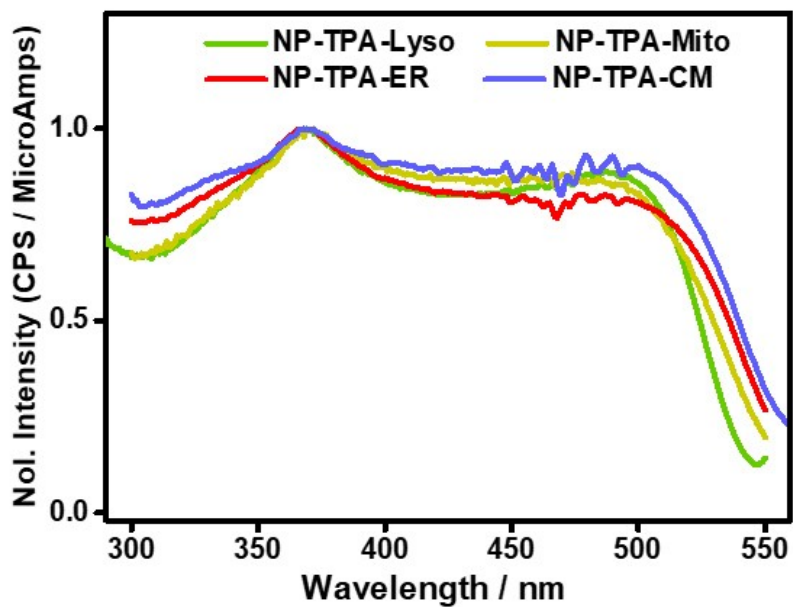


Fig. S6 Excitation spectrum of NP-TPA-Tars in solid.

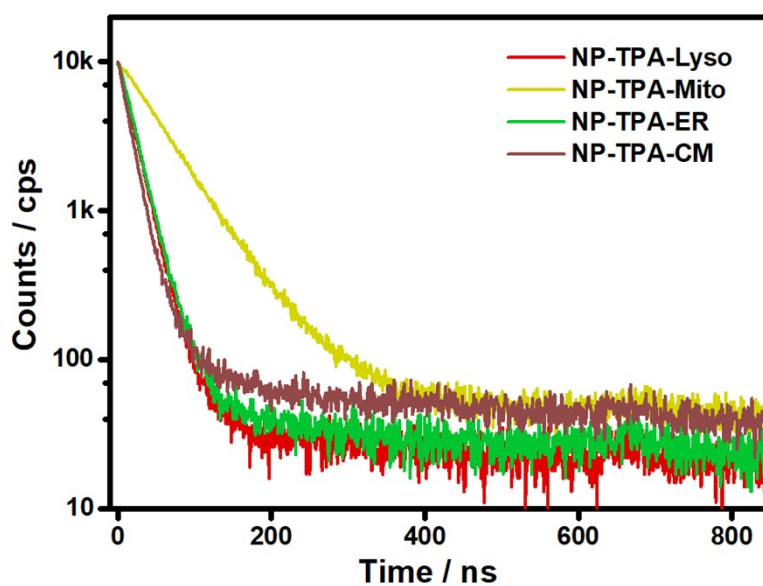


Fig. S7 Lifetime decay profiles of NP-TPA-Tars in solid at 298 K. The fluorescence decay profiles were well-fitted using a single-photocounting method on the nanosecond time scale.

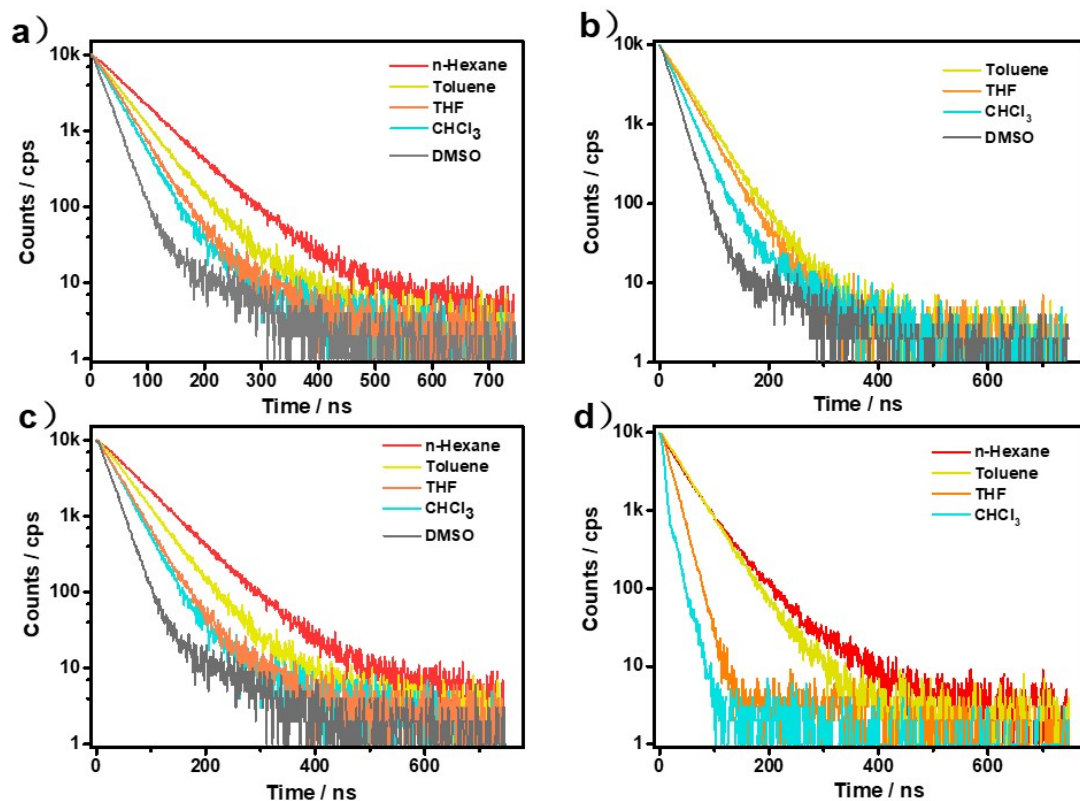


Fig. S8 Lifetime decay profiles of NP-TPA-Tars in different solvent at 298 K. (a) NP-TPA-Lyso. (b) NP-TPA-Mito. (c) NP-TPA-ER. (d) NP-TPA-CM. The fluorescence decay profiles were well-fitted using a single-photocounting method on the nanosecond time scale.

Table S1 The photophysical data for NP-TPA-Tars in solution and solid at 298 K.

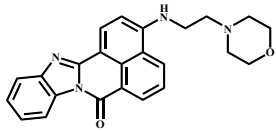
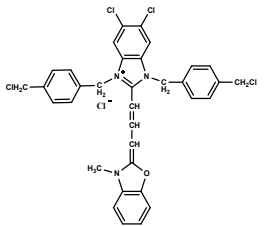
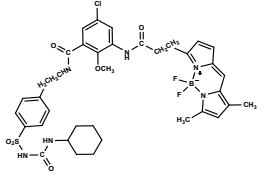
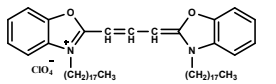
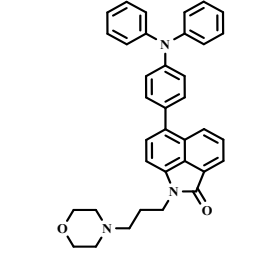
Samples		Solvents					Solid
		n-Hexane	Toluene	THF	CHCl <sub>3</sub>	DMSO	
NP-TPA-Lyso	$\lambda_{\text{abs}} / \text{nm}$	295/402	296/406	300/410	296/405	298/411	—
	$\lambda_{\text{em}}^{\text{a)}} / \text{nm}$	521	532	546	556	585	562
	$\epsilon_{\text{max}} / \text{cm}^{-1} \text{mol} \cdot \text{L}^{-1}$	79873	80412	77714	70158	73396	—
	Stokes shift /nm	119	126	136	151	174	—
	$\tau_{\text{f}}^{\text{b)}} / \text{ns}$	6.7	7.2	4.5	3.8	2.3	4.1

	$\chi^2$	1.05	1.08	1.09	1.07	1.05	1.05
	$\Phi_{\text{PL}}^{(c)} / \%$	62	51	43	25	13	71
NP-TPA-Mito	$\lambda_{\text{abs}} / \text{nm}$	—	296/413	300/417	296/406	298/411	—
	$\lambda_{\text{em}}^{(a)} / \text{nm}$	—	542	549	567	596	570
	$\epsilon_{\text{max}} / \text{cm}^{-1} \text{mol} \cdot \text{L}^{-1}$	—	119364	103449	115385	108223	—
	Stokes shift /nm	—	129	132	161	185	—
	$\tau_f^{(b)} / \text{ns}$	—	4.9	4.5	2.6	2.0	8.6
	$\chi^2$	—	1.09	1.06	1.07	1.02	1.07
	$\Phi_{\text{PL}}^{(c)} / \%$	65	52	39	28	12	68
NP-TPA-ER	$\lambda_{\text{abs}} / \text{nm}$	296/405	298/412	301/415	296/405	298/411	—
	$\lambda_{\text{em}}^{(a)} / \text{nm}$	517	526	543	578	588	572
	$\epsilon_{\text{max}} / \text{cm}^{-1} \text{mol} \cdot \text{L}^{-1}$	68554	77279	74786	76656	70174	—
	Stokes shift /nm	112	114	128	173	177	—
	$\tau_f^{(b)} / \text{ns}$	6.1	4.4	5.7	3.2	2.3	4.3
	$\chi^2$	1.08	1.00	1.00	1.08	1.07	1.09
	$\Phi_{\text{PL}}^{(c)} / \%$	68	65	58	32	18	76
NP-TPA-CM	$\lambda_{\text{abs}} / \text{nm}$	299/423	302/426	302/437	297/421	299/428	—
	$\lambda_{\text{em}}^{(a)} / \text{nm}$	575	563	585	616	—	588
	$\epsilon_{\text{max}} / \text{cm}^{-1} \text{mol} \cdot \text{L}^{-1}$	86981	87615	83888	95385	88012	—
	Stokes shift /nm	152	137	148	195	—	—
	$\tau_f^{(b)} / \text{ns}$	5.2	4.5	1.9	2.0	—	2.8
	$\chi^2$	1.04	1.03	1.01	1.01	—	1.08

	$\Phi_{\text{PL}}^{(c)} / \%$	58	42	35	21	—	72
--	-------------------------------	----	----	----	----	---	----

a) 10  $\mu\text{M}$  and  $\lambda_{\text{ex}} = 405 \text{ nm}$  for NP-TPA-Tars; b) Measured using a single-photocounting method ; c) Measured using an intergrating sphere method.

Table S2 The comparison between NP-TPA-Tars and commercial dyes.

Sample	Molecular structure	$\lambda_{\text{ex}}$ (nm)	$\lambda_{\text{em}}$ (nm)	Stokes shift (nm)	Traceable time, price	Origin
LysoGreen		443	505	62	1997, 278 ¥ / 200 $\mu\text{L}$	Commercial
Mito-Tracker Green		490	516	26	1996, 327 ¥ / 50 $\mu\text{g}$	Commercial
ER-Tracker Green		504	511	7	1997, 1303 ¥ / 20 $\mu\text{L}$	Commercial
DiO		484	501	17	1999, 472 ¥ / 10 mg	Commercial
NP-TPA-Lyso		405	585	183	—	This work

NP-TPA-Mito		405	588	183	—	This work
NP-TPA-ER		405	588	183	—	This work
NP-TPA-CM		405	615	210	—	This work

## 6. Cytotoxicity

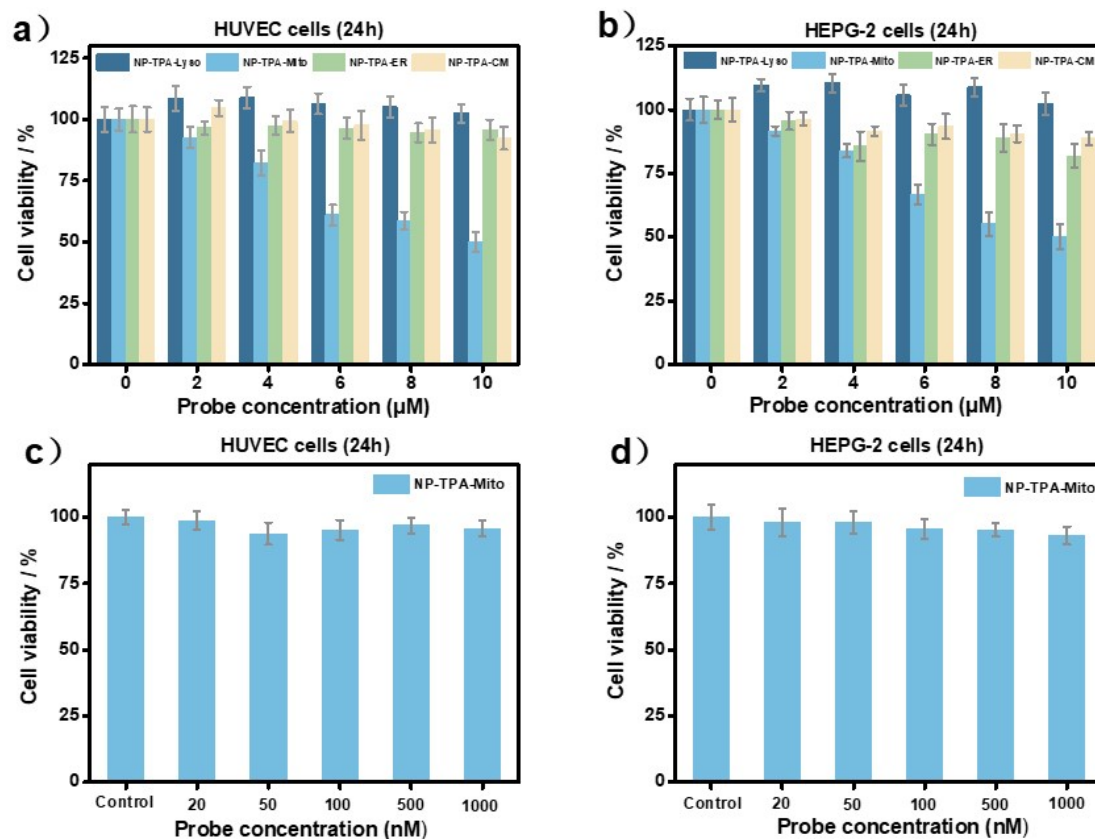


Fig. S9 Cell viability of NP-TPA-Tars after incubation with HUVEC and Hep G2 cells for 24 h in MTT assay. (a) & (b) 0-10  $\mu\text{M}$  of NP-TPA-Tar incubation with HUVEC and Hep G2 cells, respectively, (c) & (d) 0-1  $\mu\text{M}$  of NP-TPA-Mito incubation with HUVEC and Hep G2 cells, respectively. The data are taken with average and show the standard deviation ( $n = 3$ ).

## 7. Cellular imaging

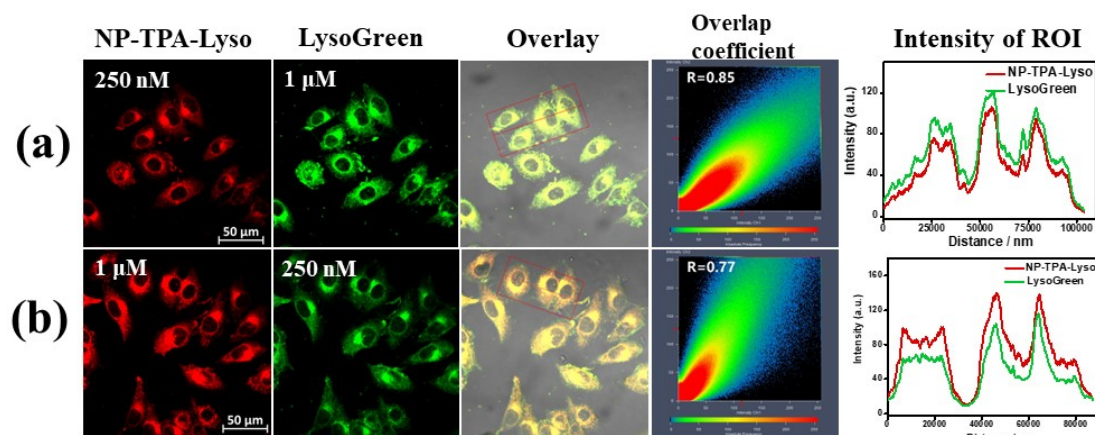


Fig. S10 Confocal fluorescence images of Hep G2 cells co-incubation with NP-TPA-Lyso ( $\lambda_{\text{ex}} = 405$



nm,  $\lambda_{em} = 590\text{--}650$  nm) and commercial dyes LysoGreen ( $\lambda_{ex} = 445$  nm,  $\lambda_{em} = 490\text{--}550$  nm). The 'Intensity of ROI' stem from the average fluorescence intensity of red outline in overlay. With different co-incubation concentrations. (a) 250 nM NP-TPA-Lyso and 1  $\mu$ M LysoGreen. (b) 1  $\mu$ M NP-TPA-Lyso and 250 nM LysoGreen.

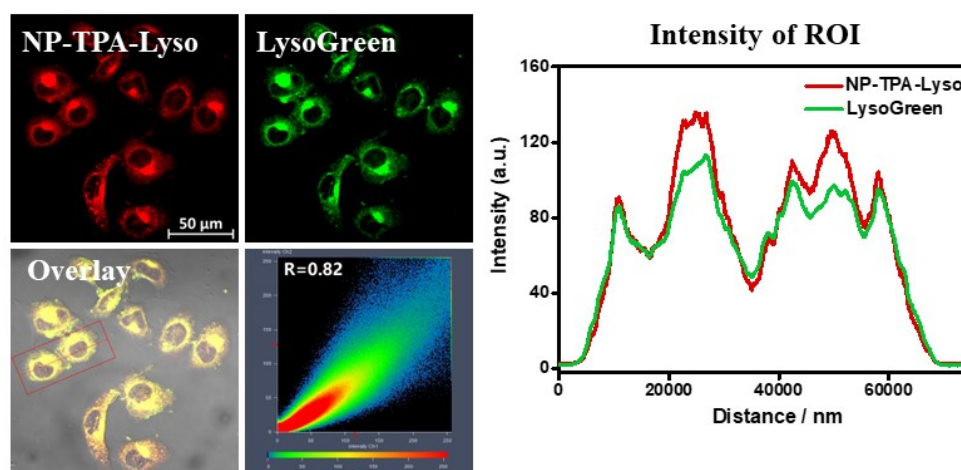


Fig. S11 Confocal fluorescence images of Hep G2 cells co-incubation with NP-TPA-Lyso and LysoGreen in same concentrations of 500 nM.

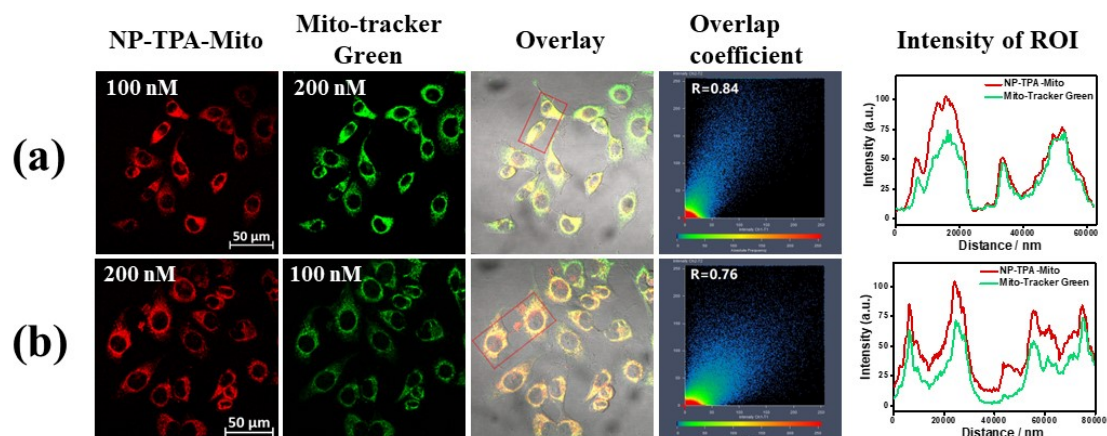


Fig. S12 Confocal fluorescence images of Hep G2 cells co-incubation with NP-TPA-Mito ( $\lambda_{ex} = 405$  nm,  $\lambda_{em} = 590\text{--}650$  nm) and commercial dyes Mito-Tracker Green ( $\lambda_{ex} = 488$  nm,  $\lambda_{em} = 490\text{--}550$  nm). The 'Intensity of ROI' stem from the average fluorescence intensity of red outline in overlay. With different co-incubation concentrations and same co-incubation time (30 min). (a) 100 nM NP-TPA-Mito and 200 nM Mito-Tracker Green. (b) 200 nM NP-TPA-Mito and 100 nM Mito-Tracker Green.

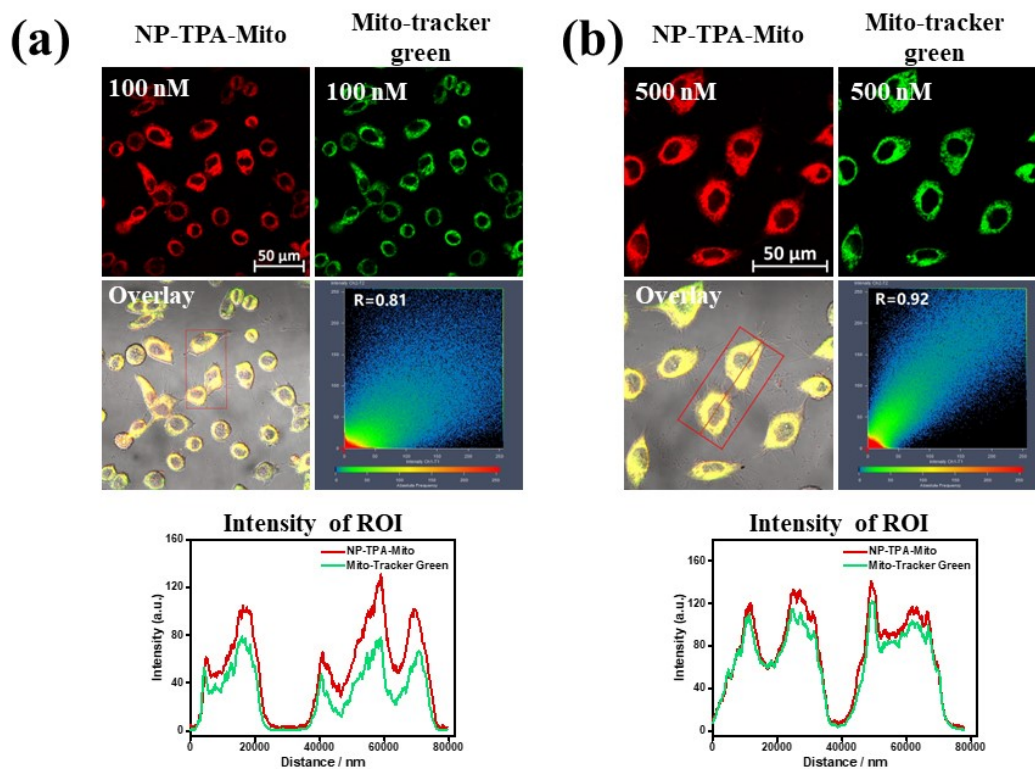


Fig. S13 Confocal fluorescence images of Hep G2 cells co-incubation with NP-TPA-Mito ( $\lambda_{ex} = 405$  nm,  $\lambda_{em} = 590-650$  nm) and commercial dyes Mito-Tracker Green ( $\lambda_{ex} = 488$  nm,  $\lambda_{em} = 490-550$  nm). The 'Intensity of ROI' stem from the average fluorescence intensity of red outline in overlay. With identical incubation concentrations. (a) 100 nM. (b) 500 nM.

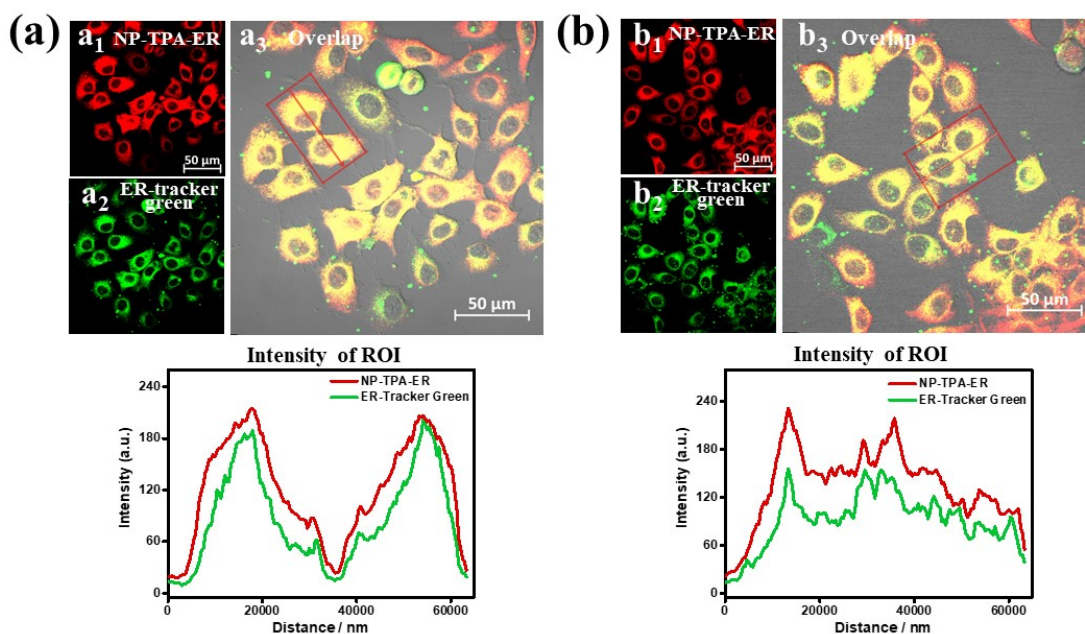


Fig. S14 Confocal fluorescence images of Hep G2 cells co-incubation with NP-TPA-ER ( $\lambda_{ex} = 405$  nm,  $\lambda_{em} = 590-650$  nm) and commercial dyes ER-Tracker Green ( $\lambda_{ex} = 488$  nm,  $\lambda_{em} = 490-550$  nm). The 'Intensity of ROI' stem from the average fluorescence intensity of red outline in overlay. With

identical incubation concentrations but different co-incubation time (50 min for NP-TPA-ER, 30 min for ER-Tracker Green). (a) 500 nM. (b) 1  $\mu$ M.

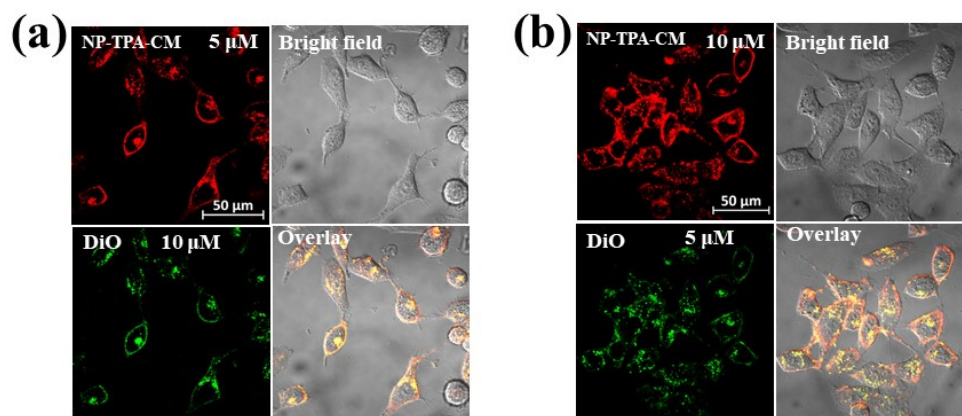


Fig. S15 Confocal fluorescence images of Hep G2 cells co-incubation with NP-TPA-CM ( $\lambda_{ex} = 405$  nm,  $\lambda_{em} = 600\text{--}650$  nm) and commercial dyes DiO ( $\lambda_{ex} = 488$  nm,  $\lambda_{em} = 490\text{--}550$  nm). With different incubation concentrations but same co-incubation time (15 min). (a) 5  $\mu$ M NP-TPA-CM, 10  $\mu$ M DiO. (b) 10  $\mu$ M NP-TPA-CM, 5  $\mu$ M DiO.

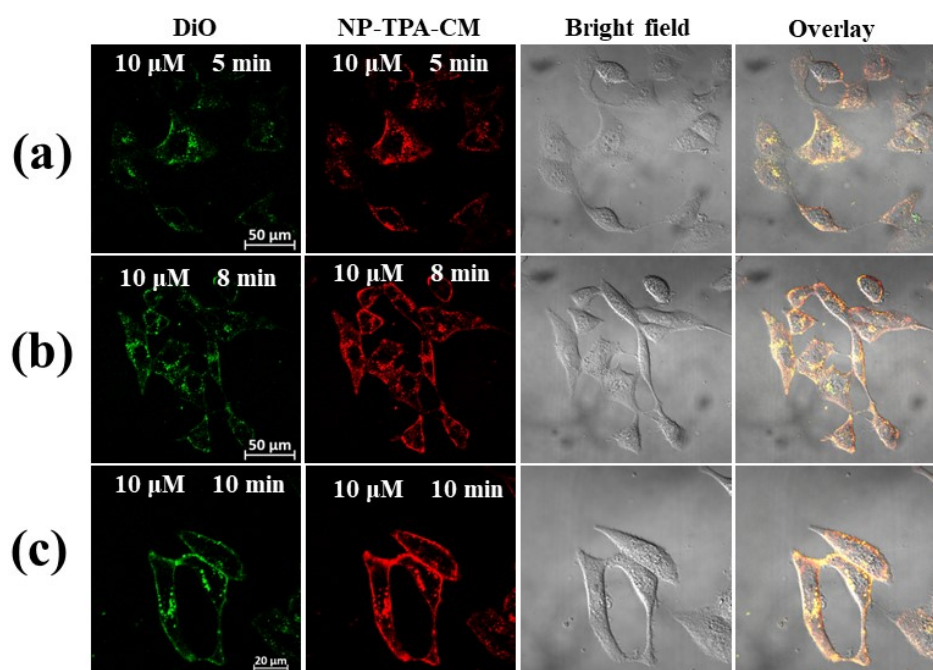


Fig. S16 Confocal fluorescence images of Hep G2 cells co-incubation with NP-TPA-CM ( $\lambda_{ex} = 405$  nm,  $\lambda_{em} = 600\text{--}650$  nm) and commercial dyes DiO ( $\lambda_{ex} = 488$  nm,  $\lambda_{em} = 490\text{--}550$  nm). With same incubation concentrations (10  $\mu$ M) but different co-incubation time. (a) 5 min, (b) 8 min and (c) 10 min.



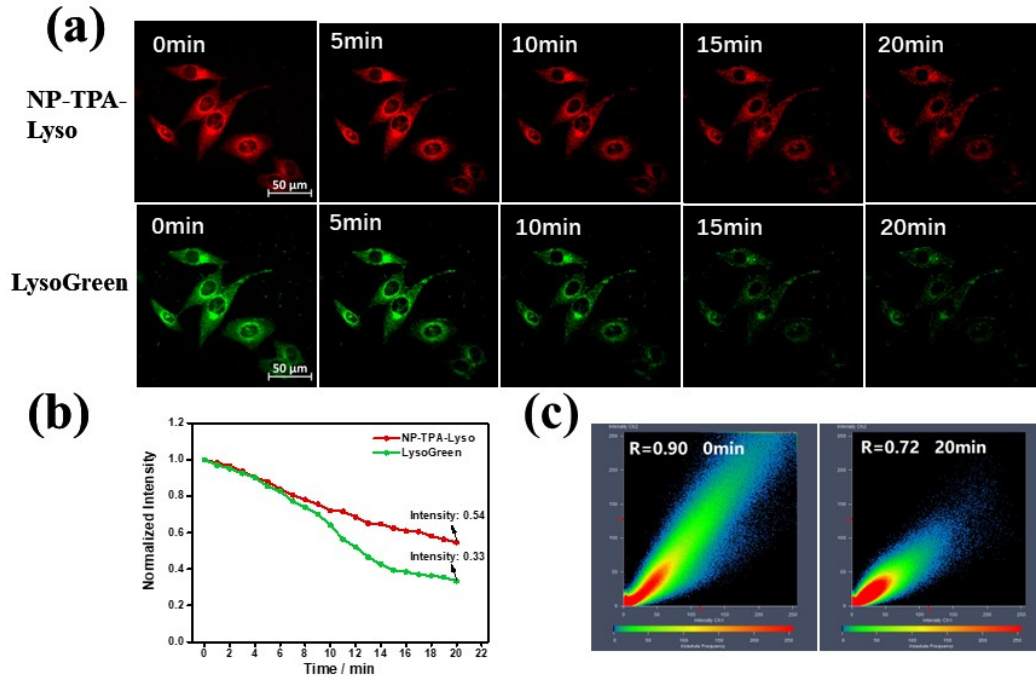


Fig. S17 Confocal fluorescence images for photostability of Hep G2 cells co-incubation 50 min with NP-TPA-Lyso ( $1 \mu\text{M}$ ,  $\lambda_{\text{em}} = 590\text{--}650 \text{ nm}$ ) and LysoGreen ( $1 \mu\text{M}$ ,  $\lambda_{\text{em}} = 490\text{--}550 \text{ nm}$ ) under laser irradiation of  $\lambda_{\text{ex}} = 405 \text{ nm}$  for 20 min. Capturing a picture every ten seconds by Zeiss LSM710. (a) The images in every five minutes captured in two channels. (b) The point line diagram of the average fluorescence intensity in every minute of NP-TPA-Lyso and LysoGreen. (c) The overlap coefficient in 0 min and 20 min of NP-TPA-Lyso and LysoGreen.

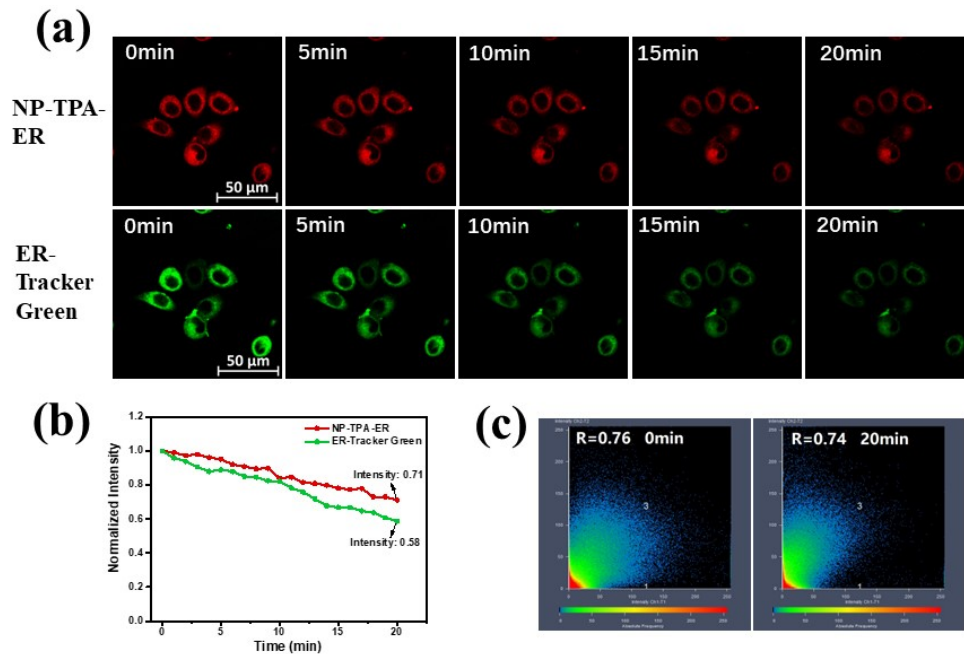


Fig. S18 Confocal fluorescence images for photostability of Hep G2 cells co-incubation with NP-

TPA-ER (1  $\mu$ M, 50 min,  $\lambda_{em}$  = 590–650 nm) and ER-Tracker Green (1  $\mu$ M, 30 min,  $\lambda_{em}$  = 490–550 nm) under laser irradiation of  $\lambda_{ex}$  = 405 nm for 20 min. Capturing a picture every ten seconds by Zeiss LSM710. (a) The images in every five minutes captured in two channels by Zeiss LSM710. (b) The point line diagram of the average fluorescence intensity in every minute of NP-TPA-ER and ER-Tracker Green. (c) The overlap coefficient in 0 min and 20 min of NP-TPA-ER and ER -Tracker Green.

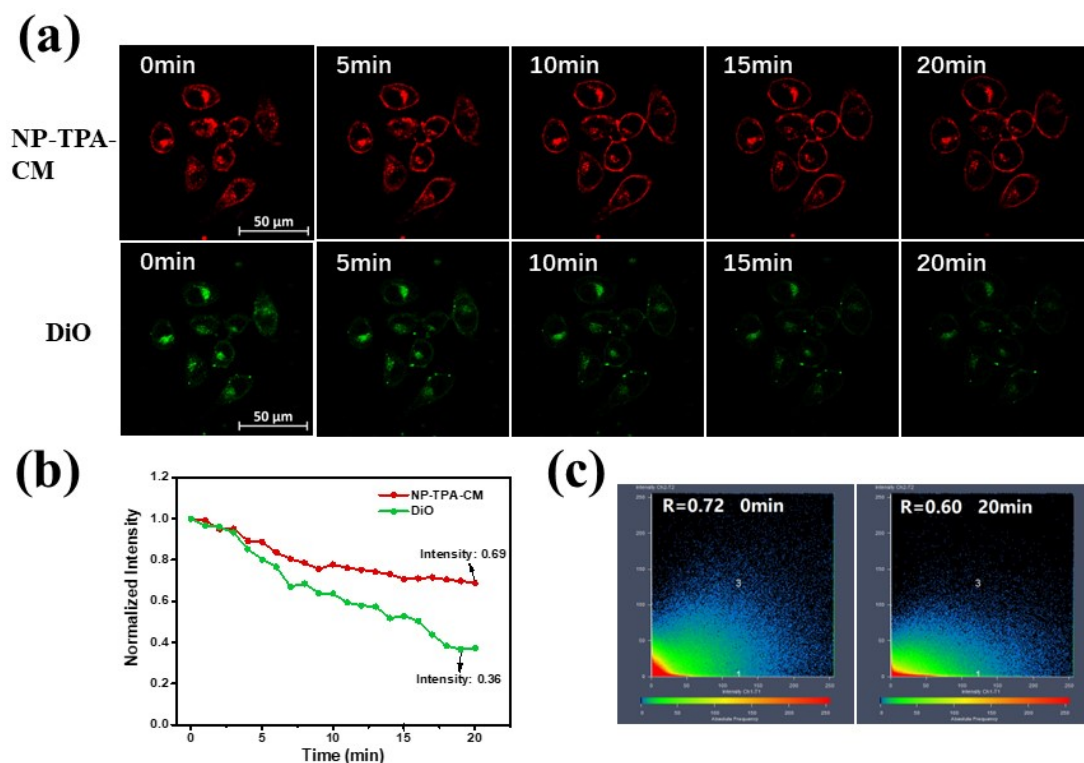
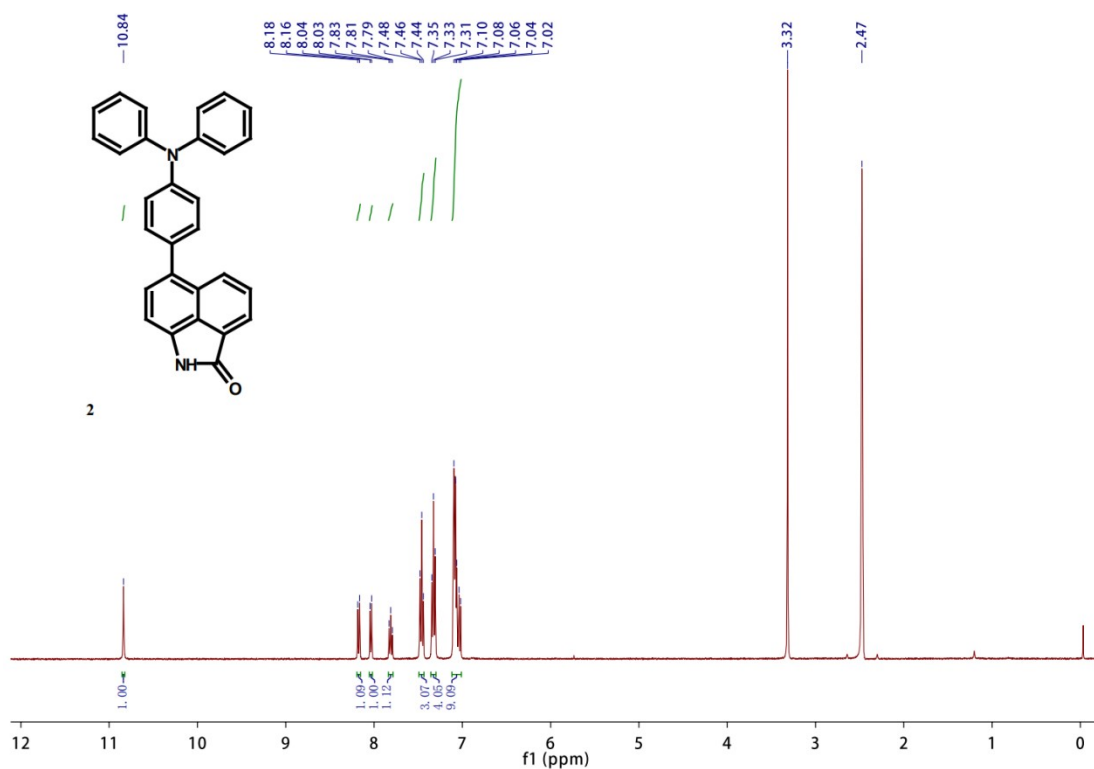
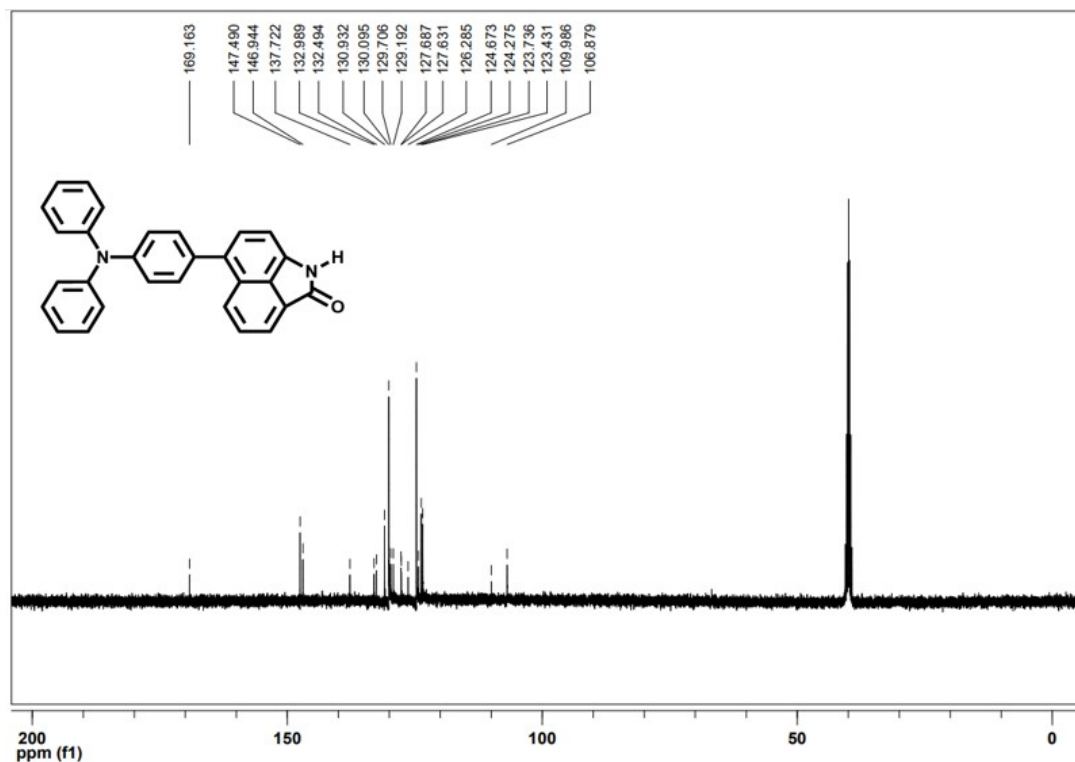


Fig. S19 Confocal fluorescence images for photostability of Hep G2 cells co-incubation 10 min with NP-TPA-CM (10  $\mu$ M,  $\lambda_{em}$  = 590–650 nm) and DiO (30  $\mu$ M,  $\lambda_{em}$  = 490–550 nm) under laser irradiation of  $\lambda_{ex}$  = 405 nm for 20 min. Capturing a picture every ten seconds by Zeiss LSM710. (a) The images in every five minutes captured in two channels. (b) The point line diagram of the average fluorescence intensity in every minute of NP-TPA-CM and DiO. (c) The overlap coefficient in 0 min and 20 min of NP-TPA-CM and DiO.

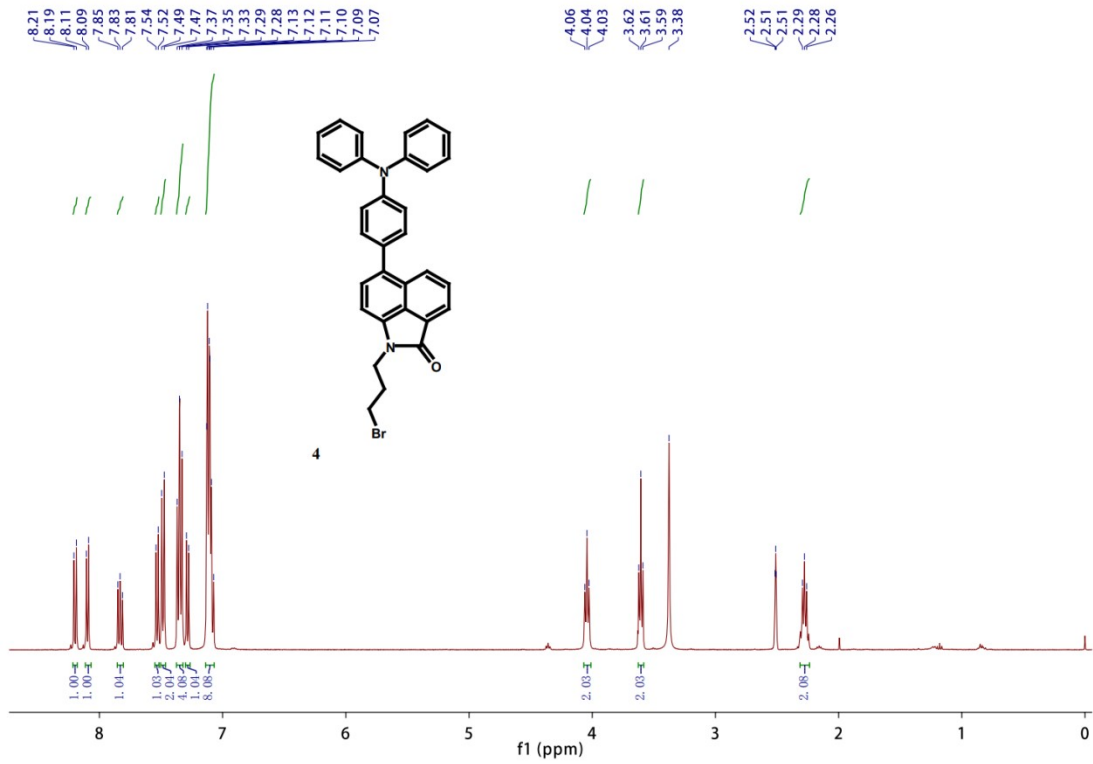
## 8. The characterization of $^1\text{H}$ NMR, $^{13}\text{C}$ NMR, and mass spectra



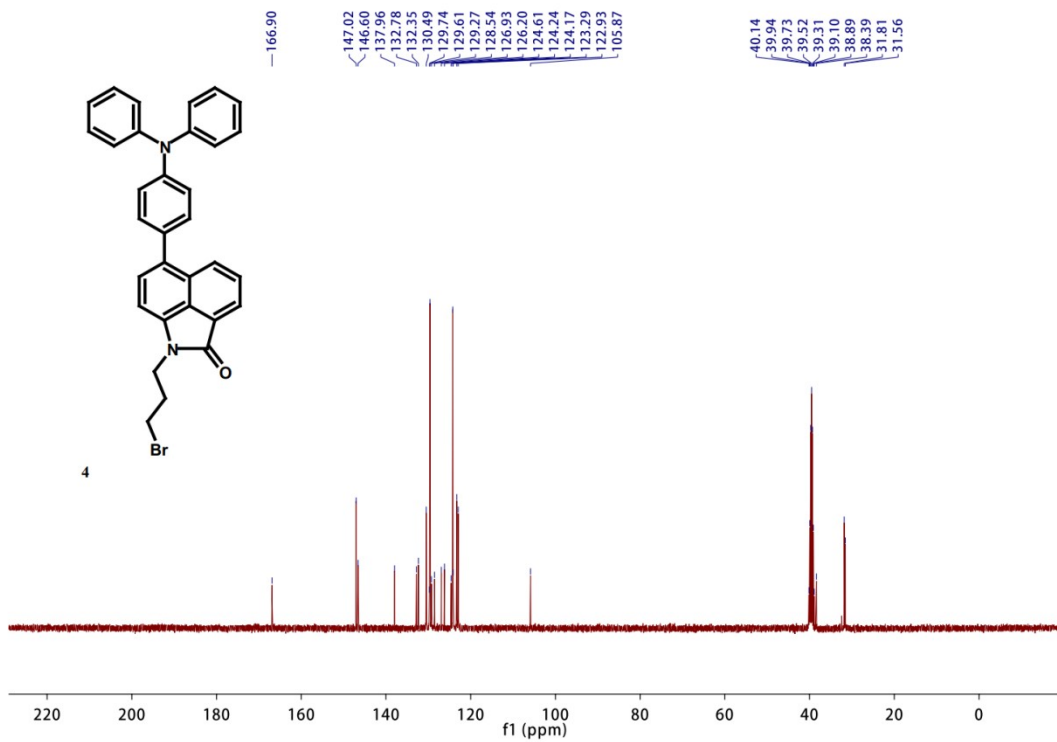
$^1\text{H}$  NMR spectrum of precursor 2 in DMSO- $d_6$ .



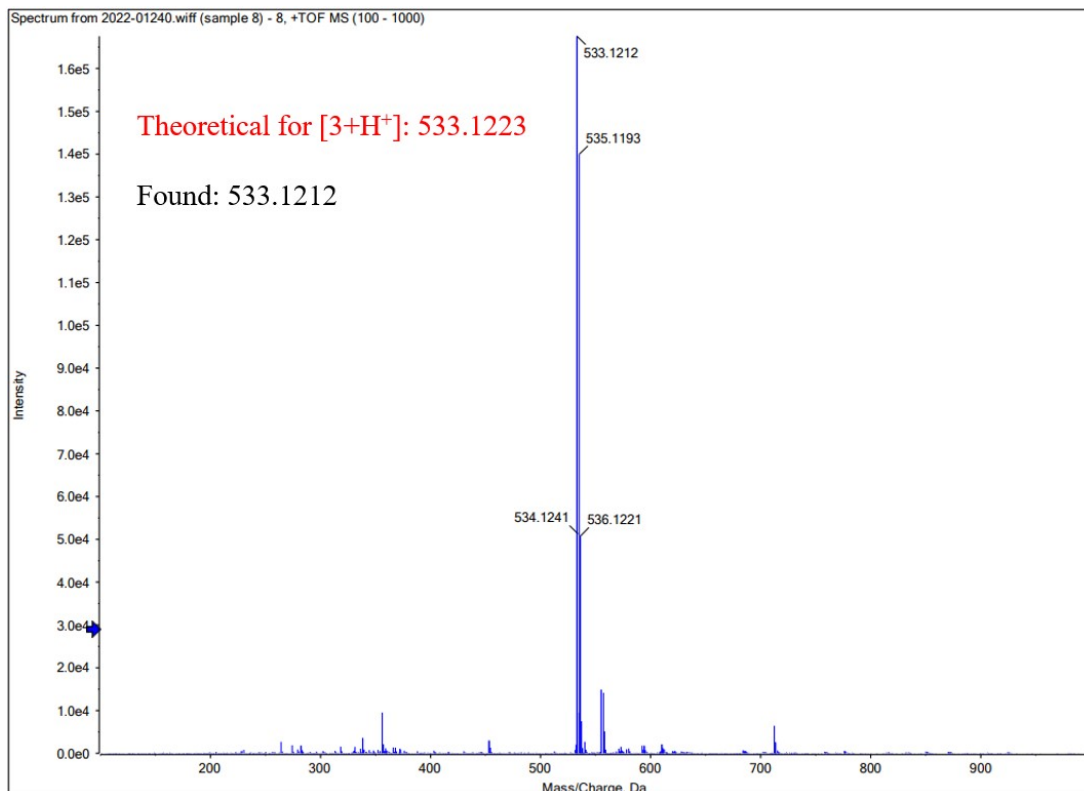
$^{13}\text{C}$  NMR spectrum of precursor 2 in DMSO- $d_6$ .



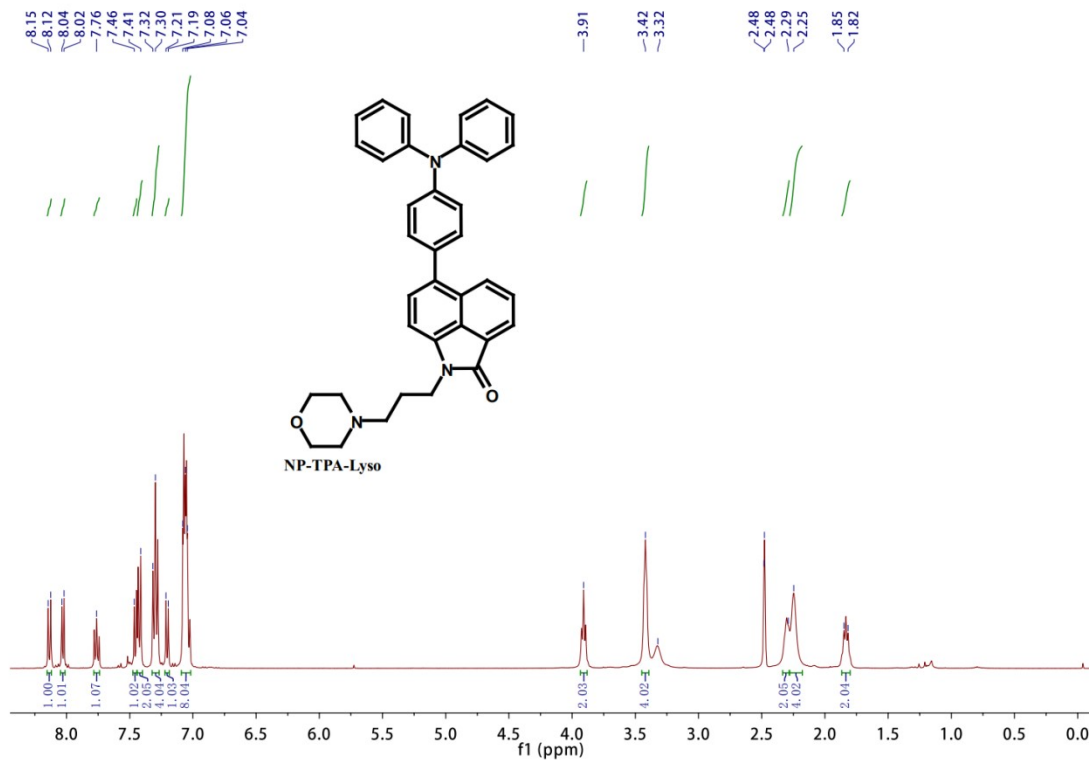
<sup>1</sup>H NMR spectrum of precursor 3 in DMSO-*d*<sub>6</sub>.



<sup>13</sup>C NMR spectrum of precursor 3 in DMSO-*d*<sub>6</sub>.

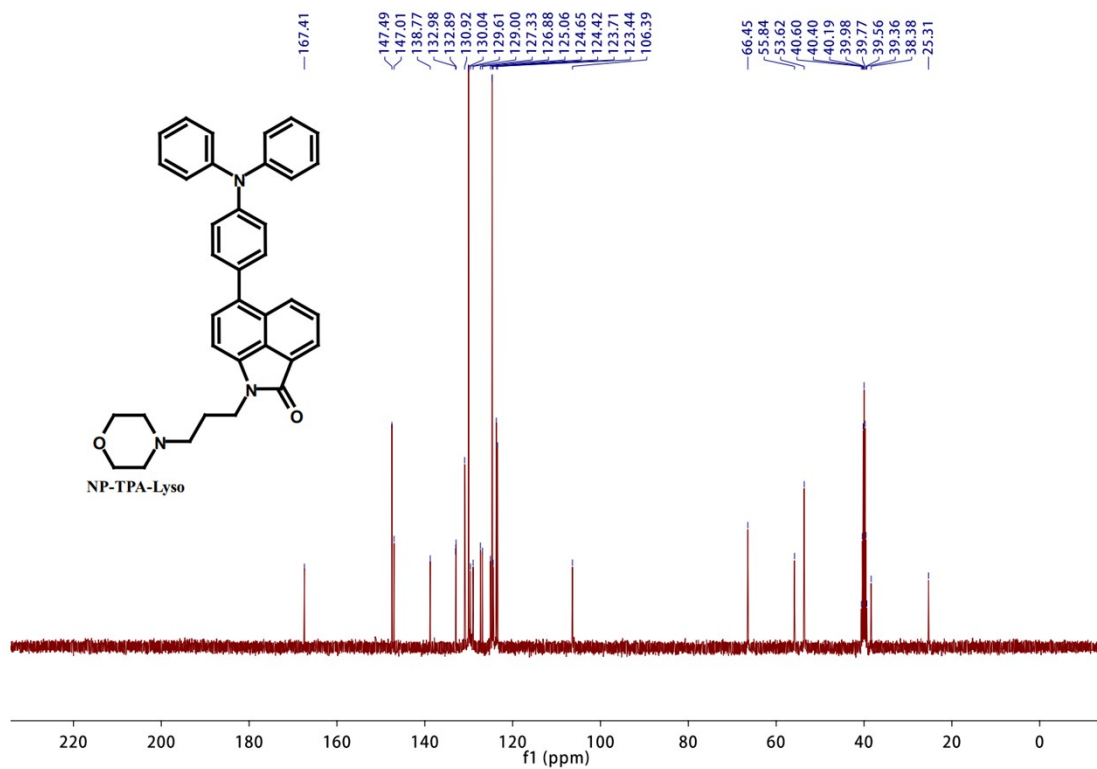


TOF-MS mass spectrum of precursor 3.

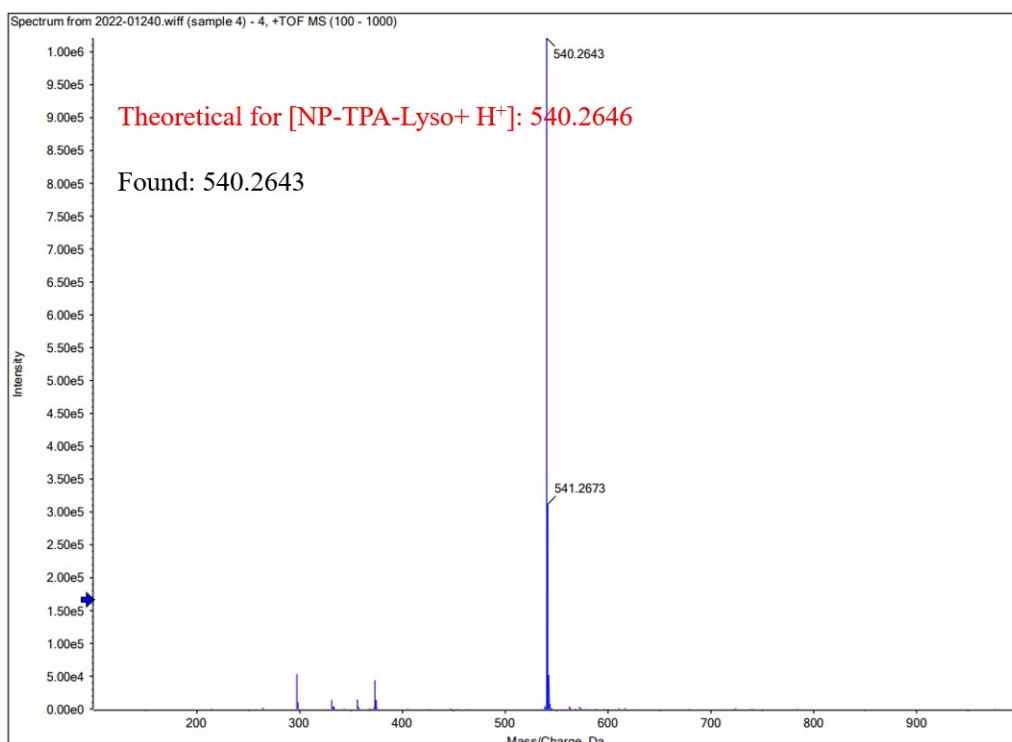


$^1\text{H}$  NMR spectrum of NP-TPA-Lyso in  $\text{DMSO-}d_6$ .

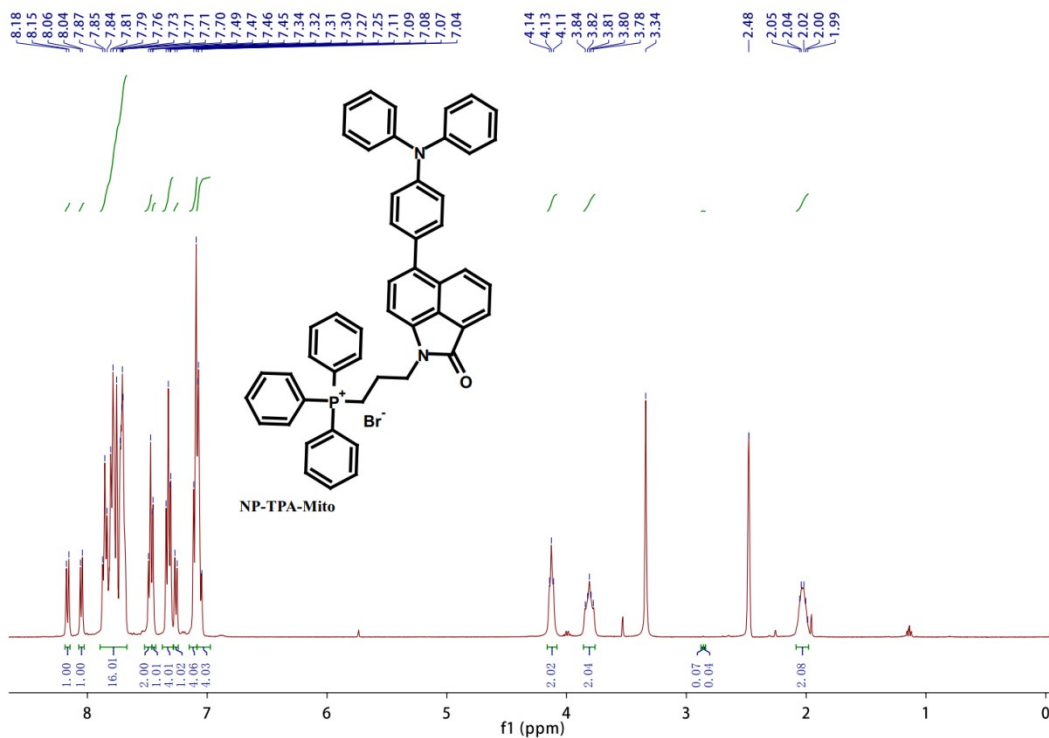




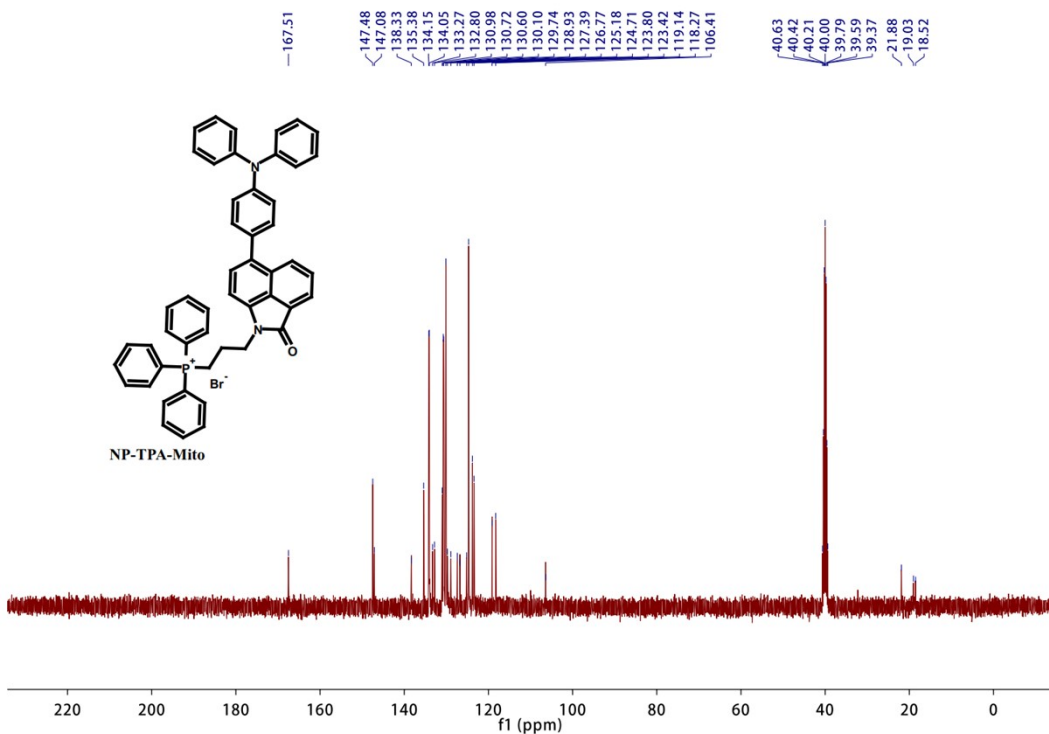
<sup>13</sup>C NMR spectrum of NP-TPA-Lyso in DMSO-*d*<sub>6</sub>.



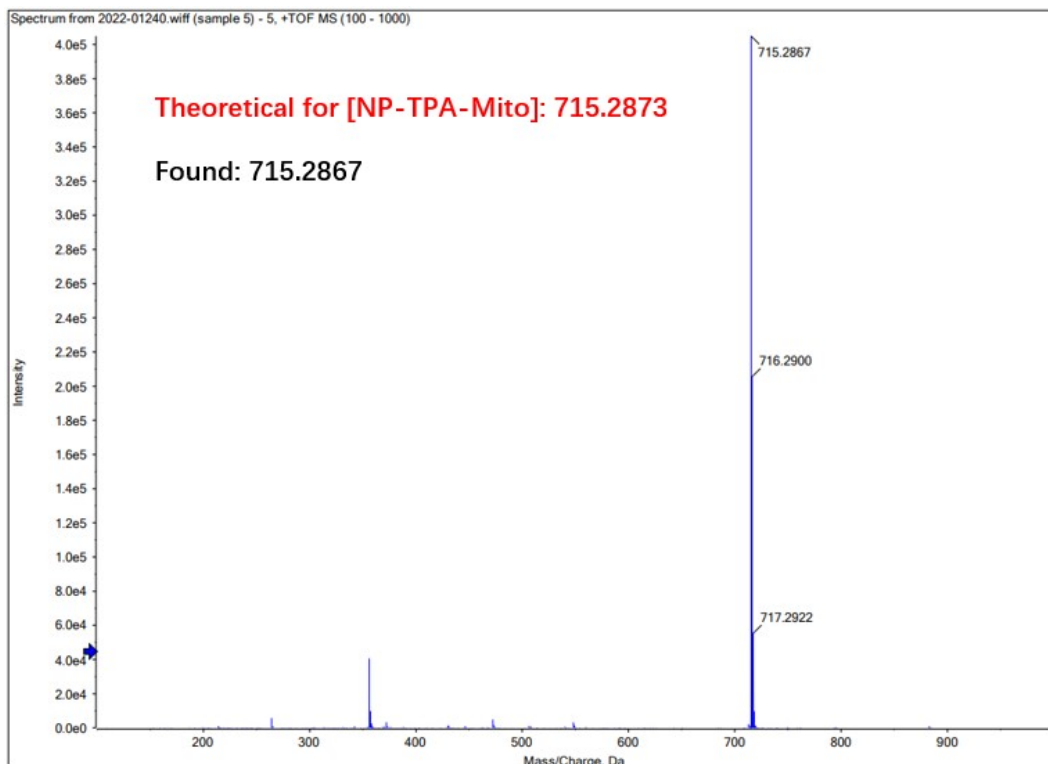
TOF-MS mass spectrum of NP-TPA-Lyso.



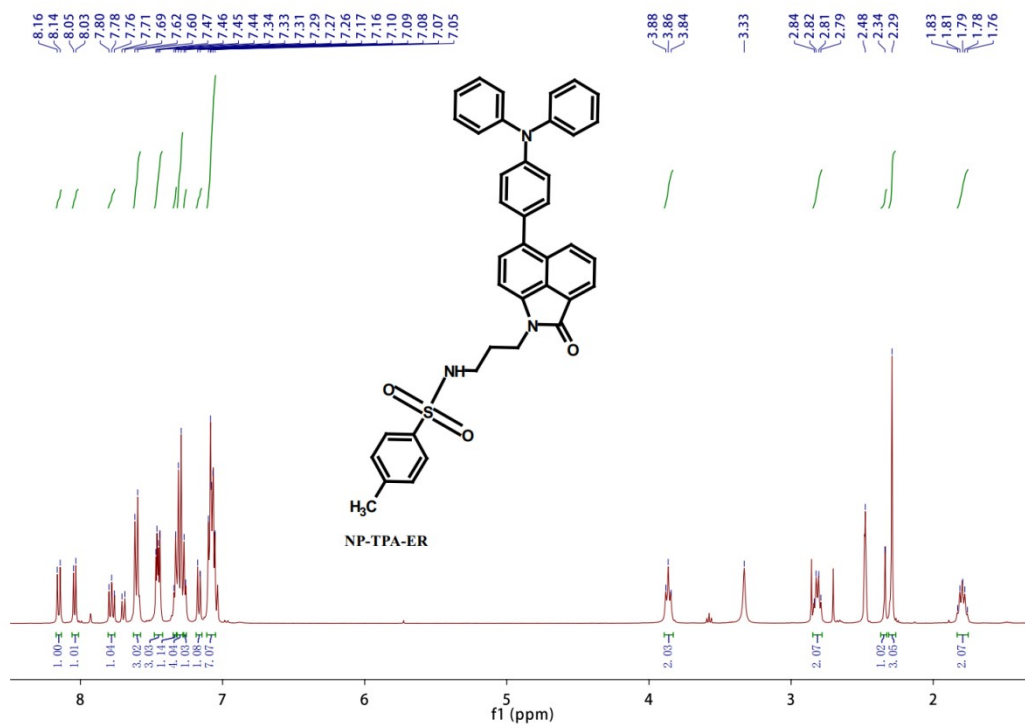
<sup>1</sup>H NMR spectrum of NP-TPA-Mito in DMSO-*d*<sub>6</sub>.



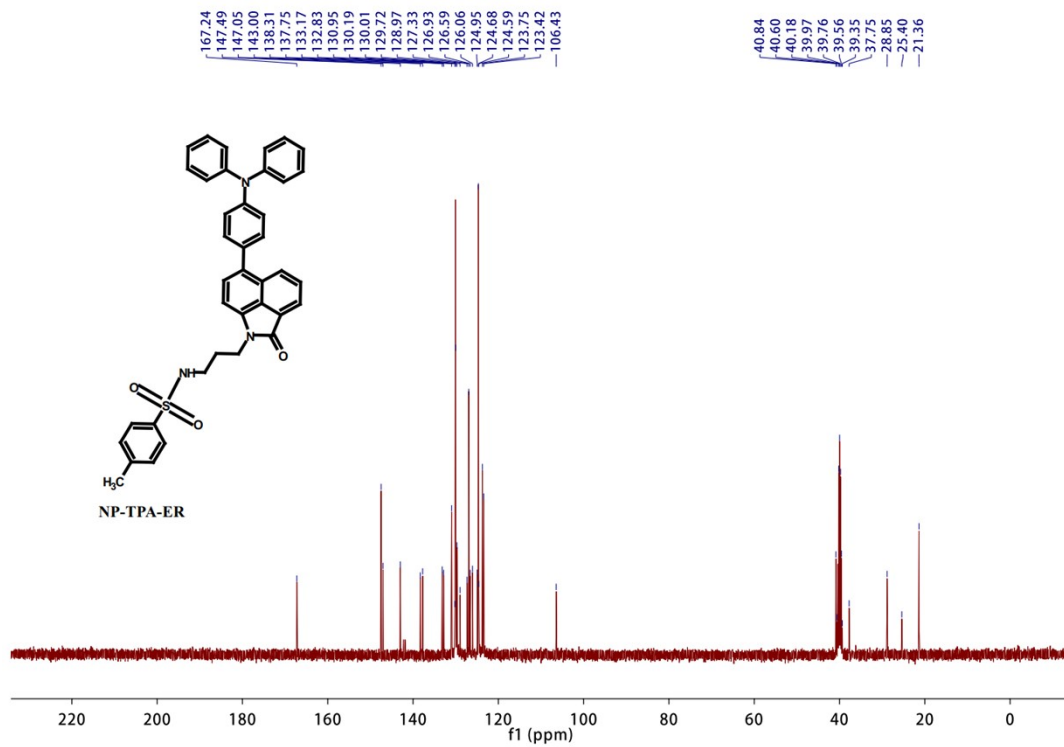
<sup>13</sup>C NMR spectrum of NP-TPA-Mito in DMSO-*d*<sub>6</sub>.



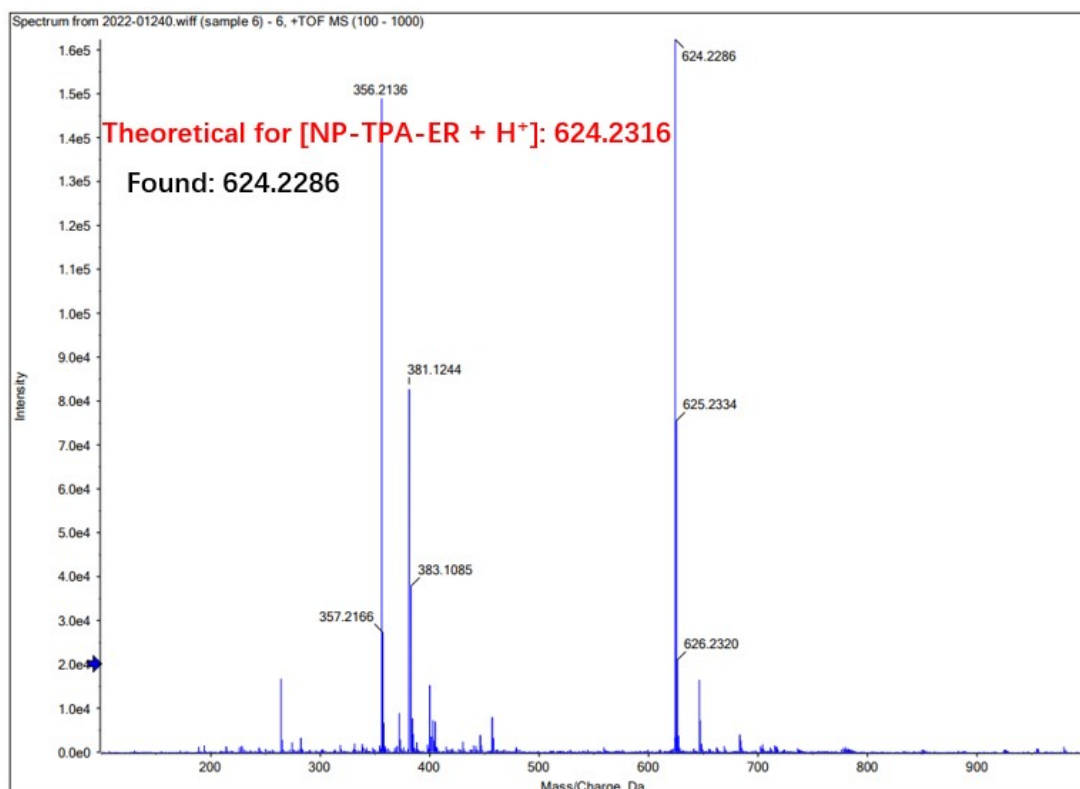
TOF-MS mass spectrum of NP-TPA-Mito.



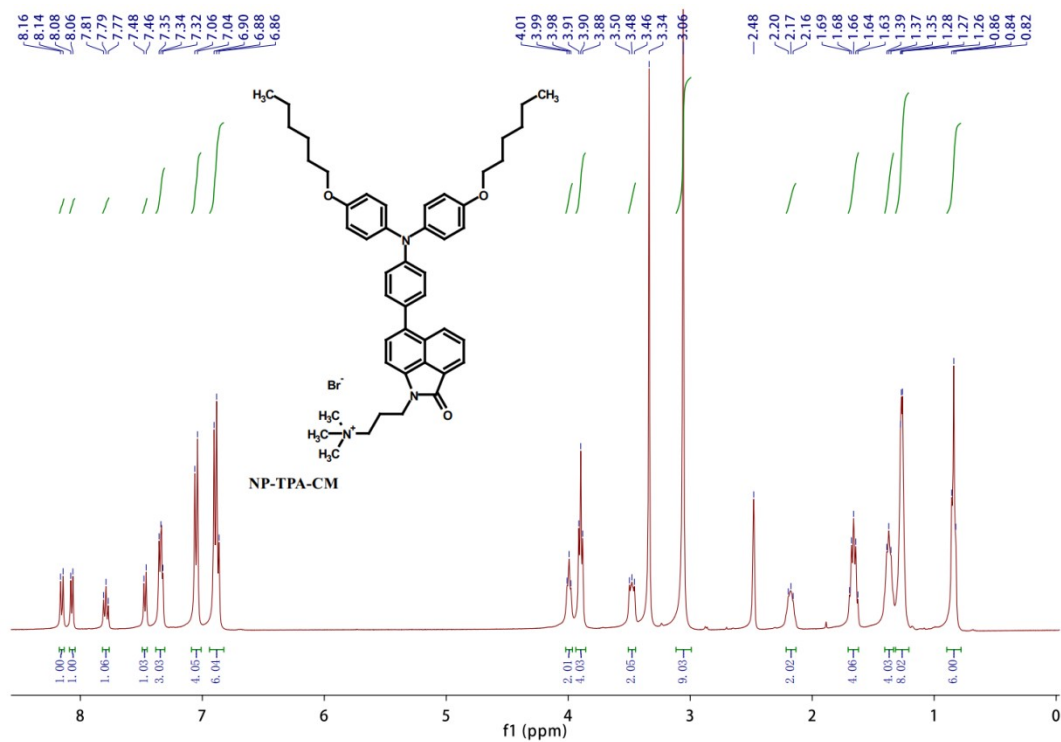
$^1\text{H}$  NMR spectrum of NP-TPA-ER in  $\text{DMSO-}d_6$ .



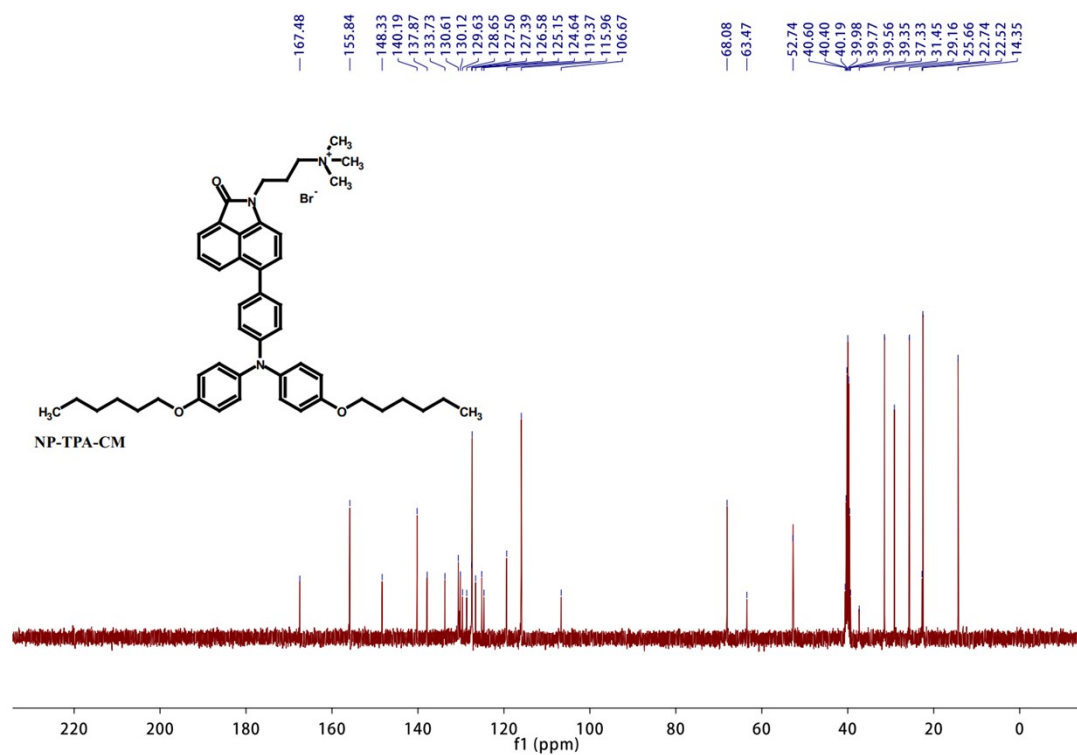
$^{13}\text{C}$  NMR spectrum of NP-TPA-ER in  $\text{DMSO-}d_6$ .



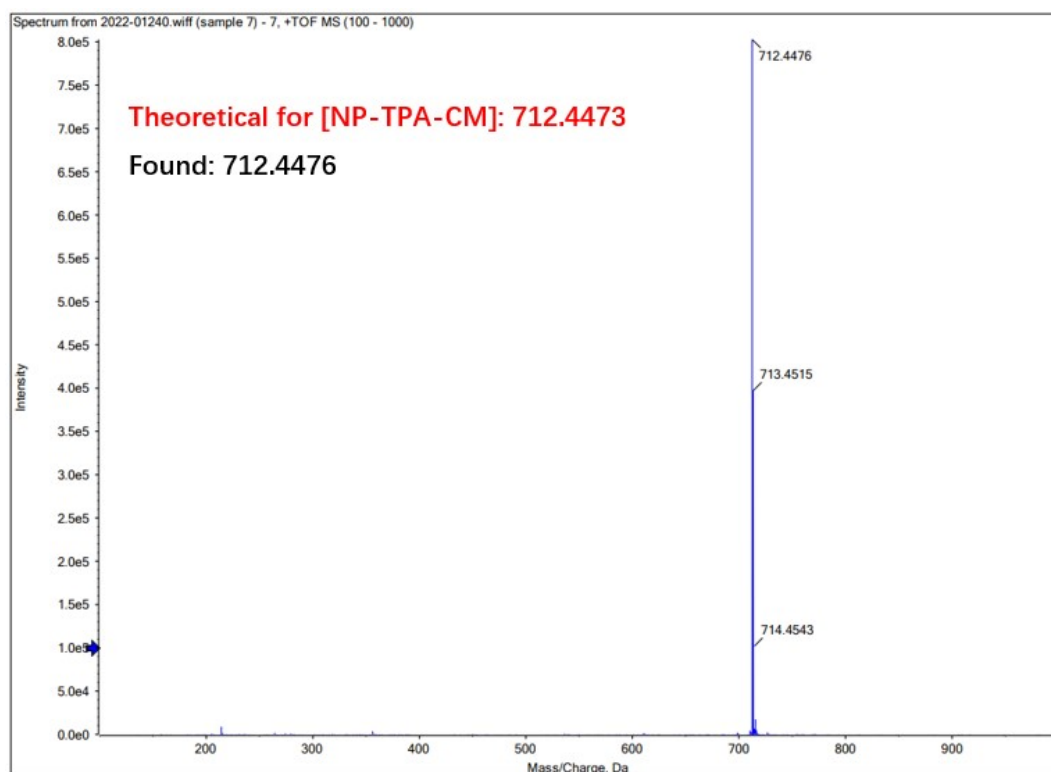
TOF-MS mass spectrum of compound NP-TPA-ER.



<sup>1</sup>H NMR spectrum of NP-TPA-CM in DMSO-*d*<sub>6</sub>.



<sup>13</sup>C NMR spectrum of NP-TPA-CM in DMSO-*d*<sub>6</sub>.



TOF-MS mass spectrum of compound NP-TPA-CM.

## 9. References

- 1 M. M. Tan, Y. Z. Li, W. H. Guo, Y. L. Chen, M. D. Wang, Y. G. Wang, B. Z. Chi, H. Wang, G. M. Xia, H. M. Wang, Accessing conjugated and twisted structures for efficient dual-state emission fluorophore and its sensitive lysosomal imaging, *Dyes Pigm.*, 2022, 201, 110243.
- 2 G. G. Ye, Y. G. Wang, L. M. Hong, F. Q. Yu, G. M. Xia, H. M. Wang, A bionic paired hydrogen-bond strategy for extending organic  $\pi$ -conjugation to regulate emission, *J. Mater. Chem. C*, 2021,9, 9142-9146.
- 3 M. F. Shah, A. Mirloup, T. H. Chowdhury, A. Sutter, A. S. Hanbazazah, A. Ahmed, J. Lee, M. Abdel-Shakour, N. Leclerc, R. Kanekoc and A. Islam, Cross-conjugated BODIPY pigment for highly efficient dye sensitized solar cells, *Sustainable Energy Fuels*, 2020, 4, 1908-1914.